University of Nevada, Reno

Spatio-temporal population dynamics of Nevada greater sage-grouse from 2000-2018

A thesis submitted in partial fulfilment of the
requirements for the degree of Master of Science in
Natural Resources and Environmental Science

by

Cheyenne R. Acevedo

Dr. Perry J. Williams/ Thesis Advisor

December, 2021

N

We recommend that the thesis
prepared under our supervision by

CHEYENNE R. ACEVEDO

entitled

**Spatio-temporal Population Dynamics of Nevada Greater
Sage-grouse from 2000-2018**

be accepted in partial fulfillment of the
requirements for the degree of

MASTER OF SCIENCE

Perry J. Williams, Ph.D.
Advisor

James S. Sedinger, Ph.D.
Committee Member

Alfred G. Schissler, Ph.D.
Graduate School Representative

David W. Zeh, Ph.D., Dean
Graduate School

December, 2021

Abstract

Dynamic spatio-temporal models, interfaced with long-term time-series data permit a better understanding of population dynamics across large spatial scales. The Greater Sage-Grouse (*Centrocercus urophasianus*) population appears to be declining across much of their range. However, there is considerable uncertainty in the spatial drivers of this decline. I developed and applied contemporary dynamic spatio-temporal statistical models to 19 years of Greater Sage-Grouse lek count data to examine spatially-explicit drivers of sage grouse population dynamics. Mean expected lek counts in Nevada declined 2.84 birds per lek between 2000 and 2018, however trends varied substantially over space, with northwestern Nevada and the Bi-State (Nevada and California) region experiencing the steepest declines (up to 6 birds per lek), and northeastern Nevada experiencing increased lek attendance. I found that elevation, total precipitation, normalized difference vegetation index, and percent sagebrush were positively correlated with expected lek counts and that drought, slope, percent bare ground, wildfire, and maximum temperatures were negatively correlated with expected lek counts. I also found that sage grouse population dynamics were closely correlated with mean precipitation the preceding 8 years. Specifically, expected lek counts tracked an eight-year precipitation average with lek attendance declining 3-4 years following 8 years of low precipitation. These results support the hypothesis that long-term mean inter-annual precipitation drives sage grouse habitat quality, and ultimately, sage grouse survival and reproduction, affecting the number of birds visiting leks the subsequent years. Finally, I provide

spatially explicit maps of population trends from 2000–2018 that can support future sage

grouse management and conservation.

I dedicate this thesis to my parents:

Catherine and Richard Acevedo

Acknowledgments

First, I would like to thank my thesis advisor, Dr. Perry Williams, for providing knowledge, perspective, and guidance during my master's degree study. Dr. Williams spent countless hours helping me achieve my goals. He taught me how to apply complex statistical methods to population modeling, answered endless questions, improved my writing, helped me troubleshoot hundreds of lines of code, and prepare for job interviews. I am thankful for all he has done to prepare me for a future career. I would also like to thank my thesis advisory committee (Dr. Alfred G. Schissler, Dr. Jim S. Sedinger, and Dr. Perry J. Williams) for providing their valuable time and expertise to my education and master's research. Dr. Schissler was an incredible resource for coding and learning the building blocks of Bayesian statistics. He was always available to answer questions and to provide support. Dr. Sedinger has been a wonderful mentor. He has an incredible knowledge base of sage grouse ecology and life history strategies that enhanced the scope of this research. They both have helped improve my writing and the way I approach the scientific thought process.

I would like the thank the Nevada Department of Wildlife for letting me use their lek count data set as well as the hundreds of volunteers, biologists, and technicians who helped collect this data. Additionally, I want to thank each person who contributed their time and provided guidance for this project (P. Coates, S. Espinosa, T. Dilts, N. Lang, and A. Matos). I am thankful for additional guidance from Dr. Alfred G. Schissler, Dr. Jim S. Sedinger, and Dr. Phillip Street regarding analyses.

I would like to thank the members of the Williams Lab (J. Brockman, and M. Byrne, S. Ellis, J. Golden, M. Keating, and M. Lohman) for their comradery, support, and intellectual understandings. Their friendships will be some of the most treasured. I would also like to thank the Sedinger lab (T. Behnke, T. Riecke, and P. Street) for their mentorship during my time as a student. They provided valuable insights and never hesitated to help me when asked.

I have spent a total of 8 years of my adult life at the University of Nevada, Reno. The interactions I've had here have shaped me as a student, a scientist, and a person. I wanted to thank everyone who has spent time teaching me, guiding me, and helping me feel included in this community. I would not be in science without all my wonderful professors, instructors, and peers. I especially want to thank Dr. Anne Leonard and Dr. Jake Francis. They took me under their wings and shaped the way I look at ecology. I attribute my enthusiasm for scientific research to them.

I would like to extend a heartfelt thank you to my friends. The friendships that endured graduate school and the ones made over the last three years will be remembered forever. I would like to acknowledge my family for their unconditional love and support, without which this achievement would not be possible. Last of all, I would like to thank my partner, James Trueblood for his love, support, and sacrifices as I completed my master's degree.

Contents

List of Tables

List of Figures

List of Appendices

1 Introduction

Anthropogenic and climatic factors are driving the worldwide degradation of grassland, rain forest, coral reef, and sagebrush ecosystems (Pandolfi et al., 2003; Bullock et al., 2020; Gang et al., 2014). Approximately 50% of the sagebrush ecosystem has experienced degradation, fragmentation, or total loss (Knick et al., 2003; Chambers et al., 2017; Mahood and Balch, 2019). This loss is the result of alterations in the landscape from anthropogenic disturbance (e.g., livestock grazing, oil and gas development, mineral extraction, agricultural conversion; Brooks and Pyke, 2001; Kulpa et al., 2012; Chambers et al., 2017), invasive species (e.g., cheatgrass; *Bromus tectorum*; Crawford et al., 2004; Wisdom et al., 2005; Freeman et al., 2014), climate change (Chambers and Pellant, 2008; Renwick et al., 2018), and altered fire regimes (D'Antonio and Vitousek, 1992; Mahood and Balch, 2019). Impacts to sagebrush habitat negatively disrupt populations that rely on them.

Greater sage-grouse (*Centrocercus urophasianus*; hereafter, sage grouse) are an indicator species for the sagebrush ecosystem, representing sagebrush quality and function (Rich and Altman, 2002; Rich et al., 2005; Suring et al., 2005; Rowland et al., 2006; Hanser and Knick, 2011). It is not surprising that as the sagebrush ecosystem has been lost, the sage grouse population has declined.

Sage grouse conservation has led to data collection programs that have amassed long-term and spatially wide-spread annual population counts during the breeding season (Jenni and Hartzler, 1978; Connelly et al., 2003; Dalke et al., 1963). These counts at

lekking locations (areas attended by sage grouse for courtship display adjacent to sagebrush dominated nesting habitat; Patterson, 1952) are used to estimate and predict population size and trends (Walsh et al., 2004; Sedinger, 2007; Blomberg et al., 2013*b*). Long-term male lek counts have declined range-wide since the 1960s (Western Association of Fish and Wildlife Agencies, 2015), and sage grouse breeding populations have declined since the 1950s (Connelly and Braun, 1997). Nevada sage grouse populations have been declining since the 1970s (Connelly et al., 2004; Lockyer et al., 2015). In 2018, Nevada Department of Wildlife (2018) estimated that Nevada lek attendance was at a 5-year low and less than the 20-year average . These declines in Nevada, and across their range, have prompted discussions to list the species under the Endangered Species Act (ESA; US Fish and Wildlife Service, 2010; Western Association of Fish and Wildlife Agencies, 2015).

Numerous factors appear to influence sage grouse population declines across many different life stages. Temperature variability influence sage grouse survival (Blomberg et al., 2014), nest or brood-rearing success (Dinkins et al., 2016), and recruitment (Blomberg et al., 2012). Warmer temperatures harm sagebrush ecosystems during vital brood-rearing periods (Blomberg et al., 2012; Miller et al., 2011), and decrease post-fledgling survival (Blomberg et al., 2014). Extreme winter weather events increase adult mortality (Moynahan et al., 2006; Anthony and Willis, 2009). Cold and wet spring weather increases chick mortality from hypothermia and malnourishment (Gregg and Crawford, 2009; Guttery et al., 2013). Drought reduces chick survival (Gibson et al., 2017). Finally, wildfire influences all life stages, where habitat loss and fragmentation are

correlated with population declines (Coates et al., 2016). These population drivers are not homogeneous in space or time.

A fundamental scientific problem is to understand the evolution of spatial processes over time (Cressie and Wikle, 2011). Although sage grouse populations appear to be declining across their range, there is considerable uncertainty about spatial variability in the drivers of population decline. In fact, in many areas in Nevada and other states, lek counts have increased through time (Gregory and Beck, 2014, Figure 1). How spatial variability behaves dynamically (i.e., the spatio-temporal variability) is key to understanding the causes of an ecological and environmental processes (Cressie and Wikle, 2011). Heterogeneity in population change permits us to understand better the drivers of the range-wide decline, and where those drivers are having the largest impact (Krebs, 1944; Wang, 2018).

Spatio-temporal statistical models are increasingly being used across many scientific disciplines to examine spatially explicit processes that evolve over time (Wikle and Hooten, 2010). Several studies have examined spatial population dynamics of sage grouse. Gregory and Beck (2014) explored the relationship between oil and gas development density and sage grouse lek attendance in Wyoming using a spatial and temporally structured analysis with geographically weighted regression to find lek attendance began to decline 1-to-4 years after disturbance from oil and gas development. McCaffery et al. (2016) developed a random effects model to examine sage grouse leks to evaluate population size, detection probability, and trend in sage grouse data collected over space and time. McCaffery et al. (2016) found the population trend in Montana decreased by 7%

per year on average. Green et al. (2017) developed a hierarchical, Bayesian state-space model to use male lek counts over 24 years to investigate the impacts of oil and gas development, and environmental and habitat conditions, on sage grouse populations. They found that precipitation the year prior to lek counts and sagebrush cover had no effect on lek counts and that male sage grouse lek attendance declined by 2.5% per year. Row and Fedy (2017) quantified the spatial-temporal cyclic dynamics of sage grouse populations using generalized additive models, wavelet and spectral analysis, and covariance analysis on male lek counts and found many regions experienced cycles, but others did not. These studies exemplify that understanding local-to-landscape level lek dynamics in a cohesive modeling framework requires advanced spatio-temporal techniques in wildlife data analysis. I aim to add to this research by creating a statistical analysis of the spatio-temporal dynamics of lek attendance in Nevada. To do this requires developing novel techniques that have not been implemented with sage grouse population counts.

In recent years there has been significant research on new statistical methodology for modeling dynamic spatio-temporal processes (Wikle and Hooten, 2010; Cressie and Wikle, 2011; Williams et al., 2017). Descriptive models (i.e., *empirical models sensu* Cressie and Wikle, 2011), such as those that have been used to examine spatio-temporal sage grouse data, address autocorrelation from the second-order (covariance) perspective (Wikle and Hooten, 2010). Descriptive models have resulted in new insights to sage grouse ecology (Gregory and Beck, 2014; Green et al., 2017; Row and Fedy, 2017), and innovative work is being done in this regard (Wikle and Hooten, 2010). However, many real-world processes are dynamic, and it can be more efficient to characterize the

spatio-temporal dependence using dynamic, first-order (mean) perspectives (Wikle and Hooten, 2010).

Dynamic spatio-temporal statistical (DSTMs) models permit predictions in space, forecasting in time, assimilation of observations and non-linear mechanistic models, and accounting for conditional dependence in parameter estimation (Wikle and Hooten, 2010; Cressie and Wikle, 2011). DSTMs consist of modeling current values of a process at a location in space to evolve from past values of the process at varying locations (Cressie and Wikle, 2011). By allowing processes to evolve conditionally, we can study how the process changes over time as well as the spatial pattern of change or growth of a system over time. Although sage grouse population dynamics have been studied widely across their range, in several states, and by a number of agencies and institutions (Connelly et al., 2003; Connelly and Schroeder, 2007), I seek methods that permit continuous spatial inference on population dynamics and how those have evolved through time. Dynamic spatio-temporal models, interfaced with long-term population time-series data have permitted a better understanding of population dynamics across large spatial scales for many species. Examples include house sparrows (*Passer domesticus*; Wikle, 2003), Eurasian collared doves (*Streptopelia decaocto* Hooten et al., 2007), wild turkey (*Meleagris gallopavo* Wang, 2018), and sea otters (*Enhydra lutris* Williams et al., 2017, 2018, 2019; Lu et al., 2020; Eisaguirre et al., 2021).

My objective was to develop a DSTM to permit predictions of sage grouse lek attendance in Nevada through time, as well as provide inference on the controlling parameters of the processes that govern lek attendance (Wikle and Hooten, 2010; Wikle,

2003). I used a long-term (2000–2018) data set of lek attendance collected in Nevada, USA. I address multiple questions regarding sage grouse population dynamics, including 1) estimating annual expected lek attendance for Nevada, 2) estimating the spatial dynamics of lek attendance in Nevada, 3) identifying the exogenous drivers behind the spatial dynamics, and 4) understanding the local or landscape features that promote expected lek attendance. Additionally, I develop a spatio-temporal map describing regions where populations in Nevada have increased, and conversely, regions where populations have decreased.

2 Methods

2.1 Study Area

The Great Basin is 541,730 km^2 and one of the largest intact sagebrush ecosystems in the world, making it critical to sage grouse conservation. Nevada is 286,382 km^2 and comprises ~50% of the Great Basin. I used the data collected at 1,980 known sage grouse leks in Nevada (see *Data Collection* section and Figure 1). Nevada's Great Basin Desert consists of rugged mountains oriented from north to south, flat valleys, and sandy desert regions (Elliott, 1987). Elevation ranges from 914 m to 4,007 m (Western Regional Climate Center, 2021). Nevada is an arid landscape, receiving on average 18 cm of precipitation per year. Nevada's water sources depend heavily on snow melt and spring precipitation (Western Regional Climate Center, 2021). Average summer temperatures range from $10°$ C to $44°$ C, and average winter temperatures range from $2°$ C to $18°$ C

(Elliott, 1987). Vegetation communities in Nevada's Great Basin vary considerably

according to elevation (Miller et al., 2011). Vegetation consists of salt desert (shadscale),

sagebrush grassland, pinyon-juniper woodland, mountain shrub, sub-alpine forest, and

alpine tundras (Germano and Lawhead, 1986; Chambers et al., 2007). Sage grouse leks

are found in areas with low, sparse vegetation, with higher amounts of bare ground,

surrounded by and adjacent to sagebrush habitats (Scott, 1942; Patterson, 1952;

Klebenow, 1985; Bradbury et al., 1989).

2.2   Data Collection

The Nevada Department of Wildlife (NDOW), in partnership with federal agencies

including the Bureau of Land Management (BLM), U.S. Forest Service (USFS), U.S.

Geological Survey (USGS), the U.S. Fish and Wildlife Service (USFWS), and citizen

volunteers, surveyed approximately 40% of the 1,980 known sage grouse leks annually

between 2000 and 2018 (Nevada Department of Wildlife, 2018). I considered all lek count

data collected in Nevada between 2000 and 2018. Lek surveys typically occur between

March and May (Connelly et al., 2003). However, depending on weather and winter

conditions, males will begin displaying in January and continue until June (Schroeder

et al., 1999; Connelly et al., 2003, 2004). The Nevada Department of Wildlife surveyed

leks as early as January in some years of the study.

      To minimize variability in lek counts associated with timing, weather conditions,

and other factors that affect sage grouse behavior or observer ability, lek counts were

conducted using the established protocol described in Connelly et al. (2003). Briefly, these

methods consisted of surveyors arriving at the lek 45 minutes before sunrise. Surveyors maintained a distance of >200 yards from leks to prevent disturbing sage grouse. All counts took place between 30 minutes before sunrise and 1.5 hours after sunrise. When possible, leks were observed from vehicles due to sage grouse being less sensitive to a vehicle's approach and presence than a person (Patterson, 1952). Surveyors obtained a minimum of three counts at 15-minute intervals of each lek on each date surveyed. Each interval consisted of a count of males, females, and birds with an undetermined sex status. To account for confounding variables during lek counts, wind direction, wind speed, temperature, ground condition, and cloud cover were recorded at the time of the survey. Not all leks were sampled every year. If leks were sampled multiple times during the breeding season, surveys at the same lek took place at least one week apart. Aerial surveys used helicopters flown at altitudes that minimized disturbance to sage grouse (Nevada Department of Wildlife, 2018). Data collected between 2000 and 2018 followed these standardized protocols, and therefore, I used these data for the analysis.

2.3 Data filtering

I used male sage grouse counts because they are the most consistent metric and observers often fail to record females due to low detection probabilities (Connelly et al., 2003; Western Association of Fish and Wildlife Agencies, 2015). I used the monthly maximum count from replicate counts obtained during each lek survey to have one maximum lek count per lek location for each month in my analyses.

2.3.1   2000–2018 Lek Data

The number of leks surveyed in the 228 months between January 2000 and December

2018 varied widely. During the non-breeding season no leks were surveyed. On the fringe

of breeding season (i.e., January-February, May-June) fewer leks were usually surveyed

than in March and April (Appendix A). For my analysis, I only considered data from

months when there were at least 100 sage grouse counted within the month. I did this

because it resulted in a large computational savings without loss in much information.

That is, in preliminary analyses, I discovered that in months with fewer than 100 sage

grouse counted, visual examination of posterior distributions of parameter estimates were

indistinguishable from prior distributions of the corresponding parameters. Further,

examining all months with data, including months with less than 100 sage grouse counted,

resulted in slow mixing of MCMC chains and prohibitive computation time. There were

57 months between 2000–2018 in which the sum of all lek surveys yielded 100 or more

sage grouse (Appendix A, B). I used these 57 months for analysis. This precluded

modeling months when sage grouse usually do not lek (June-December) resulting in a

large computational savings. For the top 10 models (below, Table 2), I used all 57 months

of data from the *2000–2018 Lek Data* for my response variable.

2.3.2   2008–2018 Lek Data

Population size is driven by environmental conditions that precede data collection. For

example, greater amounts of precipitation prior to the sage grouse breeding season have

been linked to higher lek counts (Blomberg et al., 2012; Coates et al., 2016). Additionally,

Peebles et al. (2017) found that weather influences the number of adults on leks after a

1-year lag. Likewise, Coates et al. (2018) observed changes in population growth

following a one-year precipitation lag. Dinkins et al. (2021) found that a one and two-year

precipitation lag were positively associated with sage grouse population growth, and that a

three- and five-year fire lag model was negatively associated with abundance. I was

interested in 1-8 year environmental lags to examine the fine to longer scale impacts on

expected lek counts. To examine models with temporal *lag effects* (e.g., lag models 1-17

below, Table 5), I subset the 57 months of the Nevada lek data to include only the months

that existed between 2008–2018. There were 37 months between 2008–2018 that

contained at least 100 sage grouse counted per month. Restricting the time frame of the

data to 2008–2018 permitted me to examine the correlation between lek counts during

2008–2018 and the environmental conditions in the 8 years preceding lek counts. Many of

the environmental covariates in my analyses (e.g., monthly burn area, and normalized

difference vegetation index) were not available in years 1992-1999.

2.4   Hypotheses linking lek attendance to exogenous variables

I examined environmental, climatic, vegetative, and disturbance covariates in a set of

conceptual models relating lek dynamics to environmental variables. Elevation, slope,

percent bare ground cover (Rigge et al., 2020), percent sagebrush cover, and water were

static in time(Table 1). Monthly precipitation, monthly maximum temperature, fire

frequency, normalized difference vegetation index (NDVI), and Palmer Drought Severity

Index (PDSI) were dynamic in time (Table 1). I created candidate models with different

combinations of static and dynamic covariates based on existing literature and experience (Table 2).

My first hypothesis was that expected lek counts were positively correlated with elevation due to increased precipitation, essential vegetation, water sources, and cover (Billings, 1951; Chambers et al., 2014; Baxter et al., 2017). My second hypotheses was that slope was negatively correlated with expected lek counts because sage grouse appear to select flat areas during breeding (Beck, 1977; Knick et al., 2013; Baxter et al., 2017). Lek locations have been shown to be positively correlated with bare ground (Scott, 1942; Petersen, 1980; Klebenow, 1985; Bradbury et al., 1989). Therefore, my third hypothesis was that bare ground cover would be positively correlated with expected lek counts (Fremgen et al., 2016). My fourth hypothesis was that percent sagebrush cover (*Artemisia spp.*) would be positively correlated with expected lek counts due to lek locations being adjacent to sagebrush habitat with adequate cover for breeding and nesting (Patterson, 1952; Gibson, 1996; Connelly et al., 2004). My fifth hypothesis was that water bodies are positively correlated with lek counts because access to water is critical to sage grouse recruitment (Atamian et al., 2010; Connelly et al., 2011; Donnelly et al., 2018). My sixth hypothesis was that monthly precipitation would be positively correlated with expected lek counts because early spring precipitation increases soil moisture, amount of vegetation for cover, and nesting habitat around lek locations (Connelly et al., 2004, 2011; Blomberg et al., 2012; Fremgen et al., 2019). My seventh hypothesis was that maximum monthly temperature is negatively correlated with lek counts because high temperatures ultimately ends breeding, driving movements away from leks into summer ranges (Pratt et al., 2017).

Additionally, high temperatures reduces female survival during the breeding season (Dinkins et al., 2017). My eighth hypothesis was that expected lek counts will decrease with fire frequency due to reduced sagebrush habitat quality (Connelly et al., 2000a, 2004; Coates et al., 2016; Foster et al., 2019). My ninth hypothesis was that NDVI is positively correlated with expected lek counts because greater NDVI is positively associated with sage grouse population growth and recruitment (Blomberg et al., 2012) and selected by sage grouse at all reproductive stages (Dinkins et al., 2014). My tenth hypothesis was that PDSI is positively correlated with expected lek counts. PDSI ranges from -10 (dry) to 10 (wet), and therefore, I expect dryer areas to have lower sagebrush quality (Aldridge et al., 2008).

2.5   Hypotheses linking lek attendance to past fire frequency

I examined the impact of fire frequency within a one-year, two-year, four-year, and eight-year time frame on expected lek counts. I chose multiple time frames for fire frequency because it is relatively unknown how long after a fire the sage grouse population is affected, or how wildfire affects lek attendance. Wildfire has been shown to impact sage grouse winter, nesting, and brood-rearing habitat for 10 to 30 years (Hanna et al., 2015; Foster et al., 2019; Blomberg et al., 2012). I calculated the lag covariates for fire frequency as the sum of the number of fires in each $10km \times 10km$ grid cell for the lag period. For example, the expected lek counts in a grid cell in January of 2008 would be predicted by the total number of fires in that grid cell during 2007 when using a one-year fire frequency lag model. I hypothesized a one-year fire lag may have no impact on sage

grouse lek counts due to high fidelity to breeding areas (Dalke et al., 1963). I also believed that a two and four-year fire lag may decrease lek counts, due to reduced nest success and recruitment from the fire-impacted area. I hypothesized that an eight-year fire lag would be negatively associated with expected lek counts because areas with many fires the preceding 8 years will have had a large cumulative effect on the number of birds in the population, and may supersede lek fidelity.

2.6   Hypotheses linking lek attendance to past precipitation

I used the PRISM Monthly Spatial Climate Data set AN81m, defined as the total monthly precipitation (including rain and melted snow), to examine the relationship between lek counts and precipitation (Daly et al., 2015). I examined the impacts of mean precipitation during a one, two, three, four, five, and eight-year period on lek counts. I chose these time frames to compare to other studies reporting positive impacts of precipitation lag effects on sage grouse populations (Blomberg et al., 2012; Coates et al., 2016; Peebles et al., 2017; Coates et al., 2018; Dinkins et al., 2021). The sagebrush ecosystem is limited by moisture, and precipitation is a driver of vegetation change and composition (Lauenroth and Sala, 1992; Bates et al., 2006; Davies et al., 2011). Weather can impact reproductive success in sage grouse and have delayed effects (Blomberg et al., 2012; Guttery et al., 2013; Blomberg et al., 2014; Caudill et al., 2014; Gibson et al., 2017). Peebles et al. (2017) showed that weather had a one-year lag effect on adult numbers on leks. Lek counts increased the following year after a wet, cool brood-rearing period. The lag covariates for precipitation were calculated as the average precipitation in each

$10km \times 10km$ grid cell for the duration of the lag period prior to lek counts. For example, the expected lek counts in a grid cell in January of 2008 would be predicted by the average precipitation in the grid cell during 2007 when using a one-year precipitation lag effect. I hypothesized that higher mean precipitation during a one, two, and. three-year precipitation lag effect would increase expected lek counts. Finally, I hypothesized that a four, five, and eight year precipitation lag effect would be correlated with lek counts because sage brush and other desert plants on which adult sage grouse rely are drought tolerant, and can sustain longer periods of drought before senescence. Thus, longer periods of sustained drought will decrease sage grouse populations and expected lek counts.

2.7   Hypotheses linking lek attendance to past drought

I used the Palmer Drought Severity Index from TerraClimate: Monthly Climate and Climatic Water Balance for Global Terrestrial Surfaces to examine the relationship between drought and lek attendance (Abatzoglou et al., 2018). Palmer drought severity is an index that measures the intensity and duration of long-term drought using precipitation, temperature, and soil moisture to estimate relative dryness (Palmer, 1965), and therefore is substantively different than the precipitation models. PDSI and precipitation are related in that PDSI uses precipitation as part of the index, but the two variables are not highly correlated. Across all time periods the correlation between the two variables had a minimum correlation of -0.603, a maximum of 0.772, and a mean of 0.104. I examined the impact of cumulative drought effects within a one, two, three, four, five, and eight-year

time frame on expected lek counts. I chose these time frames, because I was interested in the cumulative impacts drought had on sage grouse population dynamics. Aldridge et al. (2008) showed that drought conditions have negative effects on sage grouse persistence and drought during winter months reduces chick survival the following summer (Guttery et al., 2013; Gibson et al., 2017). Seasonal drought during late summer periods is associated with nutritional stress on sage grouse that can lead to negative reproductive costs (Blomberg et al., 2013c). Additionally, drought severity can influence sage grouse recruitment and individual survival by impacting available food quality during the brood-rearing period (Blomberg et al., 2012; Connelly et al., 2000b; Gregg and Crawford, 2009). I estimated the lag covariates for drought as the average PDSI in each $10km \times 10km$ grid cell. For example, the expected lek counts in a grid cell in January of 2008 would be predicted by the average PDSI in the grid cell during 2007 with a one-year drought lag model. I hypothesized a one-year, two-year, and three-year drought lag (i.e., negative PDSI values) may only have a moderate negative affect on lek counts because sage grouse females can select locations in the short term that increase chick survival during seasonal drought, therefore mitigating the impacts of drought conditions (Gibson et al., 2017). I also believed that a four-year, five-year, and eight-year drought lag will decrease expected lek counts due to lower quality sagebrush habitat with reduced plant production, cover, herbaceous vegetation, and less macro invertebrates that result from prolonged drought (Blomberg et al., 2013a; Wenninger and Inouye, 2008; Blomberg et al., 2014).

2.8 Statistical Analysis

2.8.1 Model Development

To address my hypotheses, I developed a comprehensive framework to model expected lek

counts through space and time. I used a DSTM within a Bayesian hierarchical framework

to estimate drivers of sage grouse population dynamics in Nevada from 2000-2018

(Cressie and Wikle, 2011).

Following the terminology of Berliner (1996), I present a Bayesian hierarchical

model consisting of three levels. The top-level is a *Data model* I developed to link

observed data and affiliated variation to latent ecological processes. Next, I developed

Process models to describe the underlying ecological processes (i.e., spatio-temporal

expected lek count dynamics). Finally, I developed *Parameter models* to represent the

prior knowledge about the parameter inputs in the ecological process model and data

model.

2.8.2 Data Model

I modeled lek count data as,

$$\mathbf{y}_t \sim \text{Poisson}(\mathbf{z}_t), \tag{1}$$

where $\mathbf{y}_t$ are the data (lek count data collected at every lek each year), a $1980{\times}1$ vector in

time $t = 1, \ldots, 37, \ldots, 57$ for lek location $i = 1, \ldots, 1980$. The vector $\mathbf{y}_t$ includes

information for all known lek locations in Nevada for each time period. When leks were

not surveyed, $\mathbf{y}_{i,t} \equiv 0$. The parameter $\mathbf{z}_t$ represents the expected lek counts at each lek at

time t. When leks were not surveyed, $\mathbf{z}_{i,t} \equiv 0$ and $\mathbf{y}_{i,t} = 0$ with probability equal to one.

This allowed leks that were not surveyed to have no impact on parameter estimates.

2.8.3 Process Model

To align the lek count data $\mathbf{y}_t$ to the underlying spatio-temporal ecological process, I let

$$\mathbf{z}_t = \mathbf{H}_t \boldsymbol{\lambda_t}, \tag{2}$$

where $\mathbf{H}_t$ is a 1,980×2,397 incidence matrix. That is, the incidence matrix aligns the lek

sampling design (whether a lek was surveyed in any particular year) to the Nevada study

area, which I discretized into a 51×47 grid, where each grid cell was $10km \times 10km$. I

selected the grid cell size based on balancing the improved computational demands of

larger grid cells with the improved ecological inference obtainable with smaller grid cells;

$10km \times 10km$ provided reasonable computational efficiency and was also at a scale

appropriate for estimating drivers of lek attendance. Holloran and Anderson (2005) found

that 64% of sage grouse nests were spatially distributed within 3 and 5 km of a lek. All of

the spatial units used in this analysis were measured in meters. The incidence matrix $\mathbf{H}_t$ is

populated with zeros and ones that align $\boldsymbol{\lambda}_t$ in each grid cell to the appropriate leks in that

grid cell, if the lek was surveyed that year. This also allowed different leks within the

same grid cell to have different counts $y_{i,t}$ each year, but the same expected value $\lambda_{j,t}$.

Thus, I link fine-scale lek count data, to larger scale ecological processes. The parameter $\boldsymbol{\lambda}_t$ is a 2,397$\times$1 vector that describes the spatio-temporal process driving lek counts in every grid cell, and represents the expected lek counts. To link $\boldsymbol{\lambda}_t$ to spatio-temporal covariates and spatio-temporal autocorrelation, I assumed

$$\log(\boldsymbol{\lambda}_t) = \mathbf{X}_t\boldsymbol{\beta} + \boldsymbol{\Phi}\boldsymbol{\alpha}_t, \tag{3}$$

$$\boldsymbol{\Phi} = \mathbf{Q}\boldsymbol{\Lambda}^{1/2}, \tag{4}$$

$$\mathbf{Q}\boldsymbol{\Lambda}\mathbf{Q}' = \mathbf{R}(\phi), \tag{5}$$

$$\mathbf{R}(\phi) = \mathrm{e}^{\frac{-\mathbf{D}^2}{\phi^2}}, \tag{6}$$

where $\boldsymbol{\beta}$ is a vector of estimated coefficients corresponding to the design matrix $\mathbf{X}_t$. The hypotheses described above were incorporated in the statistical model using the appropriate linear combination of design matrices and parameters, $\mathbf{X}_t\boldsymbol{\beta}$. The basis matrix, $\boldsymbol{\Phi}$, consists of columns of basis vectors resulting from the eigenvalue decomposition of a matrix in equations 4–5. The basis matrix provides a framework for estimating spatial correlation across Nevada, and correspond to a vector of estimated spatial effects, $\boldsymbol{\alpha}$ (Hefley et al., 2017). For my analysis, I selected four basis vectors to address spatial correlation. I use basis vectors because of their flexibility for approximating spatial and temporal processes (Hefley et al., 2017). The equation $\mathbf{Q}\boldsymbol{\Lambda}\mathbf{Q}'$ represents an eigenvalue decomposition that decomposes the spatial correlation function $\mathbf{R}(\phi)$ into basis values and basis vectors that are used in equation 3. The notation $\mathbf{R}(\phi)$ represents a correlation function described in equation 6. The correlation function has two components. The

parameter ϕ is a range parameter that is estimated from the data, and describes how spatial

autocorrelation decreases as distance between sites increases. $D_{j,k}$ represents the distance

among each pair of grid cells $j = 1, \ldots, 2{,}397$, in the study area. Combined, equation 6

permits us to examine how adjacent grid cells are correlated with each other, and how that

impact decreases as distance between grid cells increases.

2.8.4 Parameter Model

To complete the Bayesian specification of my model, I developed parameter (or prior)

models for each parameter. Parameters requiring prior distributions include $\boldsymbol{\alpha}_t$, $\boldsymbol{\beta}_t$, and ϕ.

Specifically, I let

$$\boldsymbol{\alpha}_1 \sim \text{Normal}(\mathbf{0}, \sigma_\alpha^2 \mathbf{I}), \tag{7}$$

$$\boldsymbol{\alpha}_t \sim \text{Normal}(\boldsymbol{\alpha}_{t-1}, \sigma_\alpha^2 dt \mathbf{I}), \text{ for } t = 2, \ldots, T \tag{8}$$

$$\boldsymbol{\beta}_t \sim \text{Normal}(\mathbf{0}, \sigma_\beta^2 \mathbf{I}), \tag{9}$$

$$\sigma_\alpha^2 \sim \text{Uniform}(0, 10), \tag{10}$$

$$\sigma_\beta^2 \sim \text{Uniform}(0, 10), \tag{11}$$

$$\phi \sim \text{Uniform}(0, 50000), \tag{12}$$

where $\boldsymbol{\alpha}_1$ is the prior for the first time period in the study and $\boldsymbol{\alpha}_t$ is the prior for time

periods $t = 2, \ldots, T$. Because $\boldsymbol{\alpha_t}$ is conditional on $\boldsymbol{\alpha_{t-1}}$, I am allowing the ecological

process of expected lek counts to evolve dynamically in space, from one time period to the

next, from a first-order (mean) perspective, constituting a DSTM. The notation dt

represents the difference in months between each sampling occurrence and the last

sampling occurrence at each location, which allows more variability to exist in $\boldsymbol{\alpha}_t$ as the

time between surveys increases. The parameter σ^2_α describes how much variability

transpires in α from one time period to the next, and $\mathbf{I}$ is the identity matrix. I chose the

prior in equation 12 because I wanted to permit enough flexibility in the estimation of

autocorrelation, such that estimates could be between approximately 0km to 100km,

conditional on $\mathbf{X}_t\boldsymbol{\beta}$ (Holloran and Anderson, 2005). I assumed 100 km (or 10 grid cells in

any direction) was the maximum, but estimates suggested spatial autocorrelation was

negligible at approximately 10 km from any grid cell.

2.9   Model Validation, Parameter Estimation, and Model Selection

I fit each of the 10 hypotheses using the model described above (and appropriate

combination of $\mathbf{X}_t\boldsymbol{\beta}$ for each model) using a custom MCMC algorithm written in R

version 3.6.2 (R Core Team, 2019, Appendix C). Before fitting the model to the Nevada

lek data, I simulated data from the hierarchical model described above, with known

parameter values. I then fit the model to the simulated data to evaluate whether the 95%

credible intervals of the approximated posterior distributions overlapped the values used

to simulate the data (Little, 2006). When fitting the model to simulated data I was able to

recover all parameters. After model validation, I fit my models to the Nevada Lek data.

For each model representing my hypotheses, I obtained two chains of 300,000 MCMC

iterations and discarded the first 200,000 as burn-in. I used a long chain and a large

amount of burn-in to permit model tuning of Metropolis-Hastings sampling. Next, I

assessed for convergence visually using trace plots and used two chains to check

Gelman-Rubin convergence diagnostics. After convergence of each model, I conducted

model checking using Bayesian p-values (Conn et al., 2018). Only models with Bayesian

p-values greater than 0.05 and less than 0.95 were considered in model selection. I

completed model selection in two stages. First, I fit all models that did not include a lag

effect (i.e., models 1 to 10) to all of the 57 months of data and calculated the Deviance

Information Criterion (DIC). Second, I used the top model from the first stage and added

additional covariates that required information up to eight years prior to the response data

(i.e., lag effects). For example, examining a model that sums up the number of fires the

previous 8 years requires having covariate data for 8 years prior to when my lek count data

first started. Coincidentally, the fire covariates I used were also first collected in 2000.

Thus, by requiring 8 years of fire data prior to the response variable data, I was required to

restrict the response data to the 37 months with more than 100 sage grouse counted

between 2008–2018 to examine the lag-effect models. Thus, I used the best model from

my first stage as a base model and created a suite of additional models with various

combinations of other lag effect covariates (models 1-17), fit each of them to the

2008–2018 lek count data, and calculated their DIC value for model comparison. I used

the model with the lowest DIC score in this second stage of model selection for all

inference (Spiegelhalter et al., 2002; Gelman et al., 2013; Hobbs and Hooten, 2015).

2.10   Derived Parameters

In addition to the parameters of the model, I derived parameters associated with sage grouse population dynamics. To examine the temporal trend at each of the 2,397 grid cells in Nevada from 2000–2018, I fit a trend line, $\gamma_{0,i}^{(k)} + \gamma_{1,i}^{(k)}t$ to the estimated expected lek counts, $\lambda_{i,t}^{(k)}$ for $t = 1, \ldots, T$ using ordinary least squares for every $k = 1, \ldots, K$ MCMC iteration. This provided posterior distributions for $\gamma_{1,i}$, permitting inference on overall increase in expected lek counts ($\gamma_{1,i} > 0$), decrease in expected lek counts ($\gamma_{1,i} < 0$), and the uncertainty in those trends (whether the 95% credible intervals of $\gamma_{1,i}$ overlap 0) from 2000-2018 for every grid cell in the study area. I also calculated the mean of $\gamma_{1,i}$ for all $i = 1, \ldots, n$ to estimate the posterior distribution of the mean trend for all Nevada from 2000-2018. Specifically, $\mu^{(k)} = \frac{1}{n} \sum_{i=1}^{n} \gamma_i^{(k)}$. Finally, I calculated the mean-squared error of the MCMC samples from the posterior distributions of $\gamma_{1,i}$ to identify areas with the most uncertainty in population trend through time. This last derivation allowed me to identify areas where we are less certain about the trajectory of Nevada sage grouse populations to target future research to reduce that uncertainty.

3   Results

Model 2 had the lowest DIC value, and thus, was the best of the candidate models in the first stage of model selection for predicting lek counts of Nevada sage grouse from 2000-2018 (Tables 2, 3). Results from model 2 suggested that expected lek counts across Nevada from 2000-2018 were positively correlated with elevation ($\beta = 0.293$, 95% CRI:

0.277,0.308), percent sagebrush (β = 0.078, 95% CRI: 0.068,0.088), NDVI (β = 0.042, 95% CRI: 0.033,0.051), and PDSI (β = 0.091, 95% CRI: 0.086,0.096). Expected lek counts were negatively correlated with slope (β = -0.354, 95% CRI: -0.362,-0.345), percent bare ground (β = -0.096, 95% CRI: -0.108,-0.085), monthly precipitation (β = -0.146, 95% CRI: -0.155,-0.138), monthly maximum temperature (β = -0.224, 95% CRI: -0.236,-0.213), and fire frequency (β = -0.005, 95% CRI: -0.015,0.0048; Table 4).

My second-stage model selection procedure examining candidate models that related lag effects to lek counts in Nevada from 2008-2018 identified the eight-year precipitation lag model as the best predictive model (Table 5). Parameter estimates for covariates included in the top model from the first-stage model-selection procedure and the second-stage model-selection procedure were in close agreement (Table 6). Additionally, my model results suggested that expected lek counts tracked the eight-year mean precipitation rate with a 3 year delay. That is, when mean precipitation over 8 years was at a minimum, expected lek counts would be at a minimum three years later, and vice versa for maximums.

The mean trend in expected lek counts in Nevada, μ, declined by 0.149 birds per lek per year (or 1 bird per lek every 6.7 years, or 2.84 birds per lek for the 2000-2018 period), although the 95% CRI overlapped zero (95% CRI: -0.538, 0.025). Expected lek counts appeared to decline everywhere in Nevada except the northeastern part of the state and few other isolated populations (Figure 4), where trend estimates were positive and had 95% CRIs that did not overlap 0, suggesting little uncertainty about the positive trend (Figure 5). In most of southern Nevada, including the Bi-State population, trend estimates

were negative and had 95% CRIs that did not overlap 0, suggesting little uncertainty about the negative trend (Figure 6). I found similar results for more local-scale populations in other parts of the state, including areas around the Sheldon National Wildlife Refuge. The estimated population trend in northwestern Nevada was negative. However, many areas had 95% CRIs that overlapped zero, suggesting uncertainty in the negative trend (Figure 6).

After restricting the data to 2008–2018, and including 8-year mean precipitation as a covariate, the mean trend in expected lek counts declined on average, but not as fast as between 2000-2018 (μ = -0.051, 95% CRI: -0.238, 0.107; Figures 4, 2).

Two areas with the most variability in the trend estimates included the Bi-State population and the population near the Sheldon National Wildlife Refuge. Despite the variability in the trends in these two locations, posterior means of trend estimates were sufficiently negative that 95% CRIs in these areas did not overlap 0. Combined, these results suggest that the populations in these areas are declining, but there is uncertainty in how fast they are declining.

4 Discussion

4.1 Trends in Nevada lek attendance 2000–2018

I estimated mean expected lek counts declined 2.84 birds per lek (0.149 birds per lek per year) between 2000 and 2018. This equates to approximately 5,600 fewer sage grouse that were expected to be counted at the 1,980 known leks in Nevada in 2018 compared to 2000.

The estimated decline is consistent with estimates obtained by the Nevada Department of Wildlife (NDOW), who have monitored 150 leks annually since 1999, and found an average decline of 2.58 birds per lek between 2000 and 2018 (0.136 birds per lek per year Nevada Department of Wildlife, 2018). The close comparison between the estimate of decrease in expected lek counts to those found in Nevada Department of Wildlife (2018) suggest that the 150 leks provide a representative estimate of lek decline statewide.

Although state-wide expected lek counts have decreased on average, they have not decreased everywhere in Nevada. Expected lek counts in northeastern Nevada (Elko County) increased by > 0.4 birds per lek per year (7.6 birds per lek between 2000 and 2018; e.g., Figure 1). The estimated increase in expected lek counts in northeastern Nevada is in contrast to Nevada Department of Wildlife (2018), who found Elko County estimates decreased by 0.42 (95%CI: -1.10–0.25) birds per lek per year, however confidence intervals in their estimate overlapped zero, suggesting the data were insufficiently precise to rule out positive trends in the area. In addition to northeastern Nevada, local populations in southeastern Nevada (White Pine and Lincoln county) appear to be increasing in trend of expected lek counts (Figure 4). While most of southeastern Nevada appears to be declining, these local populations appear to be correlated with greater NDVI values and greater percent sagebrush cover than other parts of southeastern Nevada (Figure 9).

The largest decrease in expected lek counts occurred in northwestern Nevada and the Bi-State population of the California-Nevada border (Figure 4). Here, expected lek counts decreased by > 0.6 birds per lek per year (11.4 birds per lek between 2000 and 2018;

Figure 9). The decline in the Bi-State population is consistent with findings from other

studies (Nevada Department of Wildlife, 2018). Nevada Department of Wildlife (2018)

found that from 2000-2018 the Bi-State region has exhibited a negative trend with male

lek attendance rates below the long-term average of 16.9 males per lek. In northwestern

Nevada, the decline appears most correlated with PDSI (Figure 9), which might impact

plant communities, available water sources, and wet meadows crucial to sage grouse

populations (Street, 2020; Blomberg et al., 2012; Gibson et al., 2017).

4.2   Exogenous drivers of lek attendance

Sage grouse expected lek counts were positively correlated with elevation. Leks located at

higher elevations benefit from increased amounts of precipitation, which influences

sagebrush quality in habitats surrounding leks (Fremgen et al., 2019; Blomberg et al.,

2012; Gibson et al., 2017). Higher elevations receive more precipitation, which increases

abundance of essential vegetation for sage grouse chicks during the brood-rearing period

(Blomberg et al., 2012). Higher elevations also tend to have higher levels of vegetation

composition for cover during the breeding, nesting, and brood-rearing seasons (Connelly

et al., 2011).

As hypothesized, expected lek counts decreased with slope. I attribute this to lek

locations typically occurring in flat areas with low sparse vegetation (Scott, 1942;

Petersen, 1980; Klebenow, 1985; Bradbury et al., 1989). Leks not in flat areas had smaller

lek attendance, in general. Sage grouse select winter and brood-rearing areas with flat

slopes (Beck, 1977; Connelly et al., 2003), and Dinkins et al. (2014) found that sage

grouse will select flatter locations at all reproductive stages.

Percent bare ground cover was negatively associated with expected lek counts. Previous studies have found that male sage grouse detection was negatively correlated with bare ground on leks (Fremgen et al., 2016), which could explain the decline in lek counts with increasing bare ground. I did not explicitly model detection probability, the effects of which, may manifest in the estimates of expected lek counts if non-negligible. Additionally, other studies have found that during nesting and brood-rearing, females select areas with less bare ground (Sveum et al., 1998; Lyon, 2000; Slater, 2003; Hausleitner, 2003). Areas with increased grazing pressure tend to have more bare ground than areas where grazing is excluded (Smith et al., 2018). For example, Street (2020) found that when livestock and feral horses are present at high rates there was a decline in herbaceous under-story and increased amount of bare ground at sage grouse nest and brood sites. Additionally, Hennig et al. (2021) found that percent bare ground increased with greater feral horse use. High proportions of bare ground are linked to poor soil quality (Derner et al., 2018), which can lead to increased soil erosion and exotic plant invasion (Davies and Boyd, 2019). Bare ground is susceptible to cheatgrass invasion (Jessop and Anderson, 2007), increasing the impacts of the cheatgrass fire cycle and reducing sage grouse habitat quality (Connelly et al., 2004).

Similar to other studies, percent sagebrush cover was correlated with lek counts (Connelly et al., 2000*b*, 2011; Doherty et al., 2010). I attribute this to how critical sagebrush is to sage grouse nesting, brood-rearing, and winter habitat throughout the year (Schroeder et al., 1999; Connelly et al., 2004, 2011; Kolada et al., 2009*b,a*).

Similar to Cornelis van Kooten et al. (2007), precipitation appears to be an important driver of Nevada sage grouse populations. Mean precipitation during the past eight-years was positively associated with expected lek counts in the following 3-4 years. Increased precipitation leads to increased soil moisture and results in a greater abundance of essential food resources for sage grouse such as herbaceous forbs and insects (Connelly et al., 2011; Blomberg et al., 2012; Fremgen et al., 2019). However, total precipitation amounts in sagebrush habitat have been declining, and are projected to continue to decline into the future, which may impact sage grouse habitat composition and therefore impact the number of birds on leks (Homer et al., 2015). Maximum monthly temperature was negatively correlated with expected lek counts. Warmer temperatures have been shown to drive bird movements between seasonal ranges (Pratt et al., 2017), and reduce female survival during the breeding season (Dinkins et al., 2017). Additionally, warmer maximum temperatures reduce population growth rates of sagebrush and essential vegetation throughout the year (Blomberg et al., 2012; Miller et al., 2011; Kleinhesselink and Adler, 2018), and decrease post-fledgling survival (Blomberg et al., 2014). Temperature effects may be exacerbated with increasing temperatures as climate change progresses (Homer et al., 2015). Temperatures are projected to increase in the future, impacting sagebrush quality, and increasing the influence of drought on sage grouse populations (Aldridge et al., 2008).

Sage grouse expected lek counts decreased with fire frequency. Fire has been shown to reduce sagebrush habitat quality through the altered fire frequencies from non-native plant invasions resulting in sage grouse population declines (Connelly et al., 2000*a*, 2004;

Coates et al., 2016). Fire frequency could impact the spatial distribution of expected lek

attendance (Coates et al., 2016). It has also been shown that after fire there is lower nest

and adult female survival (Foster et al., 2019), making fire frequency an important factor

to consider when examining sage grouse lek counts and population trends. The Bi-State

population appears to be negatively affected by frequent wildfires in many locations

(Figure 9), potentially driving local population declines there.

NDVI was positively associated with expected lek counts. NDVI is positively

correlated with sage grouse population growth and recruitment (Blomberg et al., 2012).

Dinkins et al. (2014) found that at all reproductive stages, sage grouse select locations

with higher NDVI values. PDSI was positively associated with expected lek counts.

Higher PDSI values are equal to higher amounts of moisture in the surrounding

environment. As PSDI values increase, the wetter the environment, and the more birds are

expected to be counted at lek locations.

4.3   Does long-term mean precipitation drive sage grouse population

cycles?

My top model suggests that sage grouse population dynamics are closely correlated with

mean precipitation the preceding 8 years. The 8-year precipitation model had much more

support from the data and spatio-temporal model than a 1-, 2-, 4- or 5-year precipitation

lag model. When the 8-year precipitation mean is at a minimum, expected lek counts in

Nevada begin to decline to a minimum in the 3-4 years following the precipitation

minimum. There are at least two potential explanations for these observations. First, high

quality sage grouse habitat is driven by long-term inter-annual precipitation, and increased plant production and macro invertebrates manifests after many years (i.e., 8 years) with above-average precipitation. Mechanistically, the high-quality habitat due to sustained periods of increased precipitation results in higher reproduction and/or survival of sage grouse, with more birds occurring at leks the in the following 3-4 years. Likewise, low-quality habitat begins to occur after 8 years of below-average precipitation, reducing survival and/or reproduction the following 3-4 years, ultimately reducing the number of birds visiting leks. Row and Fedy (2017) found that in many areas, sage grouse populations cycle over 8-9 years. My findings are consistent with the cyclic nature of the sage grouse cycle in Nevada from 2008-2018. These findings prompt future research examining the relationship between mean precipitation over an 8-year period and sage grouse population cycles in other areas of the sage grouse range.

4.4   Local features promoting expected lek attendance

All ecological processes change in space and time. However, most studies ignore space and time dependence and treat them independently or use a second-order perspective of covariation (Wikle and Hooten, 2010). In dynamic systems, for which we have rich data, using methods that permit us to model how ecological processes change dynamically through space and time permits us to address spatio-temporal variation and understand better the main drivers of population dynamics across space. By accounting for spatio-temporal autocorrelation not addressed using covariate data, we are better able to understand the realized impact of exogenous covariates on sage grouse lek dynamics.

The spatio-temporal random effects in the model show significant variation across the breading seasons from 2008-2018 (Figure 8). There is a higher amount of spatial variation during the peak months of breeding season (March-May) for each year. This could be attributed to the breeding season peaking later in the sampling months, or a higher rate of sampling effort during those months. By explicitly addressing this spatio-temporal variability in my modeling framework I was able to isolate and estimate these affects, and better understand the relationships between the covariates and lek counts, as well as, quantify the spatio-temporal variability in sage grouse counts (Figure 8). This also permits us to evaluate the variability in spatial trends in lek activity through time. For example, the Bi-State region experienced higher lek counts than predicted by the covariates in May 2009–2014, but then lower lek counts than predicted by the covariates 2015–2018. These trends capture spatial processes driven by covariates other than those included in the model.

After accounting for spatio-temporal autocorrelation, I found, as others have, a suite of exogenous drivers are affecting sage grouse populations and those drivers vary in space. In northwestern Nevada, drought appears to be the main driver of population decline (Figure 9). And while drought is similar in northeastern Nevada compared to northwestern Nevada, northeastern Nevada has had more precipitation, higher NDVI, had higher percent sagebrush than northwestern Nevada, potentially mitigating the effects of drought (Figure 9). Drought also appears correlated with the decline in expected lek counts in the Bi-State region of southwest Nevada (Figure 9). Additionally, numerous wildfires appear to be correlated with population declines in the Bi-State region (Figure 9). And while

wildfires have also occurred at high frequencies in north-central Nevada, drought has been less severe, compared to northeastern, northwestern, and southwest Nevada (Figure 9). In south-central Nevada, low levels of NDVI appear to be highly correlated with sage grouse population declines (Figure 9). The ability to weigh these driving forces of sage grouse lek attendance spatially is critical for area-based management.

4.5   Future directions and management implications

I have developed methods to understand spatio-temporal lek dynamics in Nevada, which permits us to implement best management practices at a local scale. Extending these methods to the entire sage grouse range, and improve our understanding by also interfacing demographic data to this analysis, will provide a more complete picture of how the drivers of sage grouse lek attendance affects population dynamics, as well as permit comparison of lek dynamics in Nevada to other states in the sage grouse range. These methods would permit development of range wide maps identifying the greatest threats to local and range-wide sage grouse conservation.

References

Abatzoglou, J. T., S. Z. Dobrowski, S. A. Parks, and K. C. Hegewisch. 2018. TerraClimate, a high-resolution global dataset of monthly climate and climatic water balance from 1958–2015. Scientific Data **5**:170191.

Aldridge, C. L., S. E. Nielsen, H. L. Beyer, M. S. Boyce, J. W. Connelly, S. T. Knick, and

M. A. Schroeder. 2008. Range-wide patterns of greater sage-grouse persistence. Diversity and Distributions **14**:983–994.

Anthony, R. G., and M. J. Willis. 2009. Survival rates of female greater sage-grouse in autumn and winter in southeastern Oregon. The Journal of Wildlife Management **73**:538–545.

Atamian, M. T., J. S. Sedinger, J. S. Heaton, and E. J. Blomberg. 2010. Landscape-level assessment of brood rearing habitat for greater sage-grouse in Nevada. The Journal of Wildlife Management **74**:1533–1543.

Bates, J., T. Svejcar, R. Miller, and R. Angell. 2006. The effects of precipitation timing on sagebrush steppe vegetation. Journal of Arid Environments **64**:670–697.

Baxter, J. J., R. J. Baxter, D. K. Dahlgren, and R. T. Larsen. 2017. Resource selection by Greater Sage-Grouse reveals preference for mechanically-altered habitats. Rangeland Ecology & Management **70**:493–503.

Beck, T. D. 1977. Sage grouse flock characteristics and habitat selection in winter. The Journal of Wildlife Management **41**:18–26.

Berliner, L. M., 1996. Hierarchical Bayesian time series models. Pages 15–22 *in* K. M. Hanson and R. N. Silver, editors. Maximum entropy and Bayesian methods. Kluwer Academic Publishers, Dordrecht, The Netherlands.

Billings, W. D., 1951. Vegetational zonation in the Great Basin of western North America.

Pages 101–122 *in* Les bases ecologiques de la regeneration de la vegetation des zones

 arides, volume 9. Union Internationale des Sciences Biologiques Serie B (Colloques).

Blomberg, E. J., S. R. Poulson, J. S. Sedinger, and D. Gibson. 2013*a*. Prefledging diet is

 correlated with individual growth in Greater Sage-Grouse (Centrocercus urophasianus).

 The Auk **130**:715–724.

Blomberg, E. J., J. S. Sedinger, M. T. Atamian, and D. V. Nonne. 2012. Characteristics of

 climate and landscape disturbance influence the dynamics of greater sage-grouse

 populations. Ecosphere **3**:1–20.

Blomberg, E. J., J. S. Sedinger, D. Gibson, P. S. Coates, and M. L. Casazza. 2014.

 Carryover effects and climatic conditions influence the postfledging survival of greater

 sage-grouse. Ecology and Evolution **4**:4488–4499.

Blomberg, E. J., J. S. Sedinger, D. V. Nonne, and M. T. Atamian. 2013*b*. Annual male lek

 attendance influences count-based population indices of greater sage-grouse. The

 Journal of Wildlife Management **77**:1583–1592.

Blomberg, E. J., J. S. Sedinger, D. V. Nonne, and M. T. Atamian. 2013*c*. Seasonal

 reproductive costs contribute to reduced survival of female greater sage-grouse. Journal

 of Avian Biology **44**:149–158.

Bradbury, J. W., S. L. Vehrencamp, and R. M. Gibson. 1989. Dispersion of displaying

 male sage grouse. Behavioral Ecology and Sociobiology **24**:1–14.

Brooks, M. L., and D. A. Pyke, 2001. Invasive plants and fire in the deserts of North

America. Pages 1–14 *in* K. Galley and T. Wilson, editors. The First National Congress on Fire Ecology, Prevention, and Management, San Diego, CA, Tall Timbers Research Station, Tallahassee, FL, USA.

Bullock, E. L., C. E. Woodcock, C. Souza Jr, and P. Olofsson. 2020. Satellite-based estimates reveal widespread forest degradation in the Amazon. Global Change Biology **26**:2956–2969.

Caudill, D., M. R. Guttery, B. Bibles, T. A. Messmer, G. Caudill, E. Leone, D. K. Dahlgren, and R. Chi. 2014. Effects of climatic variation and reproductive trade-offs vary by measure of reproductive effort in greater sage-grouse. Ecosphere **5**:1–11.

Chambers, J. C., J. D. Maestas, D. A. Pyke, C. S. Boyd, M. Pellant, and A. Wuenschel. 2017. Using resilience and resistance concepts to manage persistent threats to sagebrush ecosystems and greater sage-grouse. Rangeland Ecology & Management **70**:149–164.

Chambers, J. C., R. F. Miller, D. I. Board, D. A. Pyke, B. A. Roundy, J. B. Grace, E. W. Schupp, and R. J. Tausch. 2014. Resilience and resistance of sagebrush ecosystems: implications for state and transition models and management treatments. Rangeland Ecology & Management **67**:440–454.

Chambers, J. C., and M. Pellant. 2008. Climate change impacts on northwestern and intermountain United States rangelands. Rangelands **30**:29–33.

Chambers, J. C., B. A. Roundy, R. R. Blank, S. E. Meyer, and A. Whittaker. 2007. What

makes Great Basin sagebrush ecosystems invasible by Bromus tectorum? Ecological Monographs **77**:117–145.

Coates, P. S., B. G. Prochazka, M. A. Ricca, B. J. Halstead, M. L. Casazza, E. J. Blomberg, B. E. Brussee, L. Wiechman, J. Tebbenkamp, S. C. Gardner, et al. 2018. The relative importance of intrinsic and extrinsic drivers to population growth vary among local populations of Greater Sage-Grouse: An integrated population modeling approach. The Auk: Ornithological Advances **135**:240–261.

Coates, P. S., M. A. Ricca, B. G. Prochazka, M. L. Brooks, K. E. Doherty, T. Kroger, E. J. Blomberg, C. A. Hagen, and M. L. Casazza. 2016. Wildfire, climate, and invasive grass interactions negatively impact an indicator species by reshaping sagebrush ecosystems. Proceedings of the National Academy of Sciences **113**:12745–12750.

Conn, P. B., D. S. Johnson, P. J. Williams, S. R. Melin, and M. B. Hooten. 2018. A guide to Bayesian model checking for ecologists. Ecological Monographs **88**:526–542.

Connelly, J. W., and C. E. Braun. 1997. Long-term changes in sage grouse (*Centrocercus urophasianus*) populations in western North America. Wildlife Biology **3**:229–234.

Connelly, J. W., S. T. Knick, M. A. Schroeder, and S. J. Stiver, 2004. Conservation assessment of greater sage-grouse and sagebrush habitats. Western Association of Fish and Wildlife Agencies. Unpublished Report. Cheyenne, Wyoming, USA.

Connelly, J. W., K. P. Reese, R. A. Fischer, and W. L. Wakkinen. 2000*a*. Response of a

sage grouse breeding population to fire in southeastern Idaho. Wildlife Society Bulletin **28**:90–96.

Connelly, J. W., K. P. Reese, and M. A. Schroeder. 2003. Monitoring of greater sage-grouse habitats and populations. Station Bulletin 80, College of Natural Resources Experiment Station, University of Idaho, Moscow, USA.

Connelly, J. W., E. T. Rinkes, and C. E. Braun. 2011. Characteristics of greater sage-grouse habitats: a landscape species at micro and macro scales. Studies in Avian Biology **38**:69–83.

Connelly, J. W., and M. A. Schroeder. 2007. Historical and current approaches to monitoring greater sage-grouse. Monitoring populations of sage-grouse. College of Natural Resources Experiment Station Bulletin **88**:3–9.

Connelly, J. W., M. A. Schroeder, A. R. Sands, and C. E. Braun. 2000*b*. Guidelines to manage sage grouse populations and their habitats. Wildlife Society Bulletin **28**:967–985.

Cornelis van Kooten, G., A. J. Eagle, and M. E. Eiswerth. 2007. Determinants of threatened sage grouse in northeastern Nevada. Human Dimensions of Wildlife **12**:53–70.

Crawford, J. A., R. A. Olson, N. E. West, J. C. Mosley, M. A. Schroeder, T. D. Whitson, R. F. Miller, M. A. Gregg, and C. S. Boyd. 2004. Ecology and management of sage-grouse and sage-grouse habitat. Journal of Range Management **57**:2–19.

Cressie, N., and C. K. Wikle. 2011. Statistics for spatio-temporal data. John Wiley & Sons, INC., Hoboken, New Jersey.

Dalke, P. D., D. B. Pyrah, D. C. Stanton, J. E. Crawford, and E. F. Schlatterer. 1963. Ecology, productivity, and management of sage grouse in Idaho. The Journal of Wildlife Management **27**:811–841.

Daly, C., J. I. Smith, and K. V. Olson. 2015. Mapping atmospheric moisture climatologies across the conterminous United States. PLoS ONE **10**:e0141140.

D'Antonio, C. M., and P. M. Vitousek. 1992. Biological invasions by exotic grasses, the grass/fire cycle, and global change. Annual Review of Ecology and Systematics **23**:63–87.

Davies, K. W., and C. S. Boyd. 2019. Ecological effects of free-roaming horses in North American rangelands. BioScience **69**:558–565.

Davies, K. W., C. S. Boyd, J. L. Beck, J. D. Bates, T. J. Svejcar, and M. A. Gregg. 2011. Saving the sagebrush sea: an ecosystem conservation plan for big sagebrush plant communities. Biological Conservation **144**:2573–2584.

Derner, J. D., A. J. Smart, T. P. Toombs, D. Larsen, R. L. McCulley, J. Goodwin, S. Sims, and L. M. Roche. 2018. Soil health as a transformational change agent for US grazing lands management. Rangeland Ecology & Management **71**:403–408.

Didan, K., 2015. MOD13A3 MODIS/Terra vegetation indices monthly L3 global 1km SIN grid V006 (Data set) NASA EOSDIS Land Process.

Dinkins, J. B., M. R. Conover, C. P. Kirol, J. L. Beck, and S. N. Frey. 2014. Greater

    Sage-Grouse (Centrocercus urophasianus) select habitat based on avian predators,

    landscape composition, and anthropogenic features. The Condor: Ornithological

    Applications **116**:629–642.

Dinkins, J. B., M. R. Conover, C. P. Kirol, J. L. Beck, and S. N. Frey. 2016. Effects of

    common raven and coyote removal and temporal variation in climate on greater

    sage-grouse nesting success. Biological Conservation **202**:50–58.

Dinkins, J. B., K. J. Lawson, and J. L. Beck. 2021. Influence of environmental change,

    harvest exposure, and human disturbance on population trends of greater sage-grouse.

    PLoS ONE **16**:e0257198.

Dinkins, J. B., K. J. Lawson, K. T. Smith, J. L. Beck, C. P. Kirol, A. C. Pratt, M. R.

    Conover, and F. C. Blomquist. 2017. Quantifying overlap and fitness consequences of

    migration strategy with seasonal habitat use and a conservation policy. Ecosphere

    8:e01991.

Doherty, K. E., D. E. Naugle, and B. L. Walker. 2010. Greater sage-grouse nesting

    habitat: the importance of managing at multiple scales. The Journal of Wildlife

    Management **74**:1544–1553.

Donnelly, J. P., B. W. Allred, D. Perret, N. L. Silverman, J. D. Tack, V. J. Dreitz, J. D.

    Maestas, and D. E. Naugle. 2018. Seasonal drought in North America's sagebrush

    biome structures dynamic mesic resources for sage-grouse. Ecology and Evolution

    8:12492–12505.

Eisaguirre, J. M., P. J. Williams, X. Lu, M. L. Kissling, W. S. Beatty, G. G. Esslinger, J. N. Womble, and M. B. Hooten. 2021. Diffusion modeling reveals effects of multiple release sites and human activity on a recolonizing apex predator. Movement Ecology **9**:1–14.

Elliott, R. R. 1987. History of Nevada. U of Nebraska Press.

Farr, T. G., P. A. Rosen, E. Caro, R. Crippen, R. Duren, S. Hensley, M. Kobrick, M. Paller, E. Rodriguez, L. Roth, et al. 2007. The shuttle radar topography mission. Reviews of Geophysics **45**:RG2004.

Feng, M., J. O. Sexton, S. Channan, and J. R. Townshend. 2016. A global, high-resolution (30-m) inland water body dataset for 2000: first results of a topographic–spectral classification algorithm. International Journal of Digital Earth **9**:113–133.

Foster, L. J., K. M. Dugger, C. A. Hagen, and D. A. Budeau. 2019. Greater sage-grouse vital rates after wildfire. The Journal of Wildlife Management **83**:1–14.

Freeman, E. D., T. R. Sharp, R. T. Larsen, R. N. Knight, S. J. Slater, and B. R. McMillan. 2014. Negative effects of an exotic grass invasion on small-mammal communities. PLoS ONE **9**:e108843.

Fremgen, A. L., C. P. Hansen, M. A. Rumble, R. S. Gamo, and J. J. Millspaugh. 2016. Male greater sage-grouse detectability on leks. The Journal of Wildlife Management **80**:266–274.

Fremgen, A. L., C. P. Hansen, M. A. Rumble, R. S. Gamo, and J. J. Millspaugh. 2019.

Weather conditions and date influence male sage grouse attendance rates at leks. Ibis **161**:1–15.

Gang, C., W. Zhou, Y. Chen, Z. Wang, Z. Sun, J. Li, J. Qi, and I. Odeh. 2014. Quantitative assessment of the contributions of climate change and human activities on global grassland degradation. Environmental Earth Sciences **72**:4273–4282.

Gelman, A., J. B. Carlin, H. S. Stern, D. B. Dunson, A. Vehtari, and D. B. Rubin. 2013. Bayesian data analysis. CRC press.

Germano, D. J., and D. N. Lawhead. 1986. Species diversity and habitat complexity: does vegetation organize vertebrate communities in the Great Basin? The Great Basin Naturalist **46**:711–720.

Gibson, D., E. J. Blomberg, M. T. Atamian, and J. S. Sedinger. 2017. Weather, habitat composition, and female behavior interact to modify offspring survival in Greater Sage-Grouse. Ecological Applications **27**:168–181.

Gibson, R. M. 1996. Female choice in sage grouse: the roles of attraction and active comparison. Behavioral Ecology and Sociobiology **39**:55–59.

Giglio, L., C. Justice, L. Boschetti, and D. Roy. 2015. Mcd64a1 modis. Terra+ Aqua Burned Area Monthly L3 Global 500m SIN Grid V006 MCD64A1 (https://doi. org/10.5067/MODIS/MCD64A1. 006) .

Gorelick, N., M. Hancher, M. Dixon, S. Ilyushchenko, D. Thau, and R. Moore. 2017.

Google Earth Engine: Planetary-scale geospatial analysis for everyone. Remote Sensing of Environment **202**:18 – 27.

Green, A. W., C. L. Aldridge, and M. S. O'donnell. 2017. Investigating impacts of oil and gas development on greater sage-grouse. The Journal of Wildlife Management **81**:46–57.

Gregg, M. A., and J. A. Crawford. 2009. Survival of greater sage-grouse chicks and broods in the northern Great Basin. The Journal of Wildlife Management **73**:904–913.

Gregory, A. J., and J. L. Beck. 2014. Spatial heterogeneity in response of male greater sage-grouse lek attendance to energy development. PLoS ONE **9**:e97132.

Guttery, M. R., D. K. Dahlgren, T. A. Messmer, J. W. Connelly, K. P. Reese, P. A. Terletzky, N. Burkepile, and D. N. Koons. 2013. Effects of landscape-scale environmental variation on greater sage-grouse chick survival. PLoS ONE **8**:e65582.

Hanna, S., K. Fulgham, et al. 2015. Post-fire vegetation dynamics of a sagebrush steppe community change significantly over time. California Agriculture **69**:36–42.

Hanser, S. E., and S. T. Knick, 2011. CHAPTER NINETEEN. Greater Sage-Grouse as an Umbrella Species for Shrubland Passerine Birds: A MULTISCALE ASSESSMENT. Pages 475–488 *in* Greater Sage-Grouse. University of California Press.

Hausleitner, D., 2003. Population dynamics, habitat use and movements of greater sage-grouse in Moffat County, Colorado. Ph.D. thesis, University of Idaho.

Hefley, T. J., K. M. Broms, B. M. Brost, F. E. Buderman, S. L. Kay, H. R. Scharf, J. R. Tipton, P. J. Williams, and M. B. Hooten. 2017. The basis function approach for modeling autocorrelation in ecological data. Ecology **98**:632–646.

Hennig, J. D., J. L. Beck, C. J. Duchardt, and J. D. Scasta. 2021. Variation in sage-grouse habitat quality metrics across a gradient of feral horse use. Journal of Arid Environments **192**:104550.

Hobbs, N. T., and M. B. Hooten. 2015. Bayesian models: a statistical primer for ecologists. Princeton University Press.

Holloran, M. J., and S. H. Anderson. 2005. Spatial distribution of greater sage-grouse nests in relatively contiguous sagebrush habitats. The Condor **107**:742–752.

Homer, C. G., G. Xian, C. L. Aldridge, D. K. Meyer, T. R. Loveland, and M. S. O'Donnell. 2015. Forecasting sagebrush ecosystem components and greater sage-grouse habitat for 2050: Learning from past climate patterns and Landsat imagery to predict the future. Ecological Indicators **55**:131–145.

Hooten, M. B., C. K. Wikle, R. M. Dorazio, and J. A. Royle. 2007. Hierarchical spatiotemporal matrix models for characterizing invasions. Biometrics **63**:558–567.

Jarvis, A., H. Reuter, A. Nelson, and E. Guevara. 2008. Hole-Filled SRTM for the globe Version 4. Available from the CGIARSXI SRTM 90m database: http://srtm. csi. cgiar. org .

Jenni, D. A., and J. E. Hartzler. 1978. Attendance at a sage grouse lek: implications for spring censuses. The Journal of Wildlife Management **42**:46–52.

Jessop, B. D., and V. J. Anderson. 2007. Cheatgrass invasion in salt desert shrublands: benefits of postfire reclamation. Rangeland Ecology & Management **60**:235–243.

Klebenow, D. A. 1985. Habitat management for sage grouse in Nevada. World Pheasant Association Journal **10**:34–46.

Kleinhesselink, A. R., and P. B. Adler. 2018. The response of big sagebrush (Artemisia tridentata) to interannual climate variation changes across its range. Ecology **99**:1139–1149.

Knick, S. T., D. S. Dobkin, J. T. Rotenberry, M. A. Schroeder, W. M. Vander Haegen, and C. Van Riper III. 2003. Teetering on the edge or too late? Conservation and research issues for avifauna of sagebrush habitats. The Condor **105**:611–634.

Knick, S. T., S. E. Hanser, and K. L. Preston. 2013. Modeling ecological minimum requirements for distribution of greater sage-grouse leks: implications for population connectivity across their western range, USA. Ecology and Evolution **3**:1539–1551.

Kolada, E. J., M. L. Casazza, and J. S. Sedinger. 2009*a*. Ecological factors influencing nest survival of greater sage-grouse in Mono County, California. The Journal of Wildlife Management **73**:1341–1347.

Kolada, E. J., J. S. Sedinger, and M. L. Casazza. 2009*b*. Nest site selection by greater

sage-grouse in Mono County, California. The Journal of Wildlife Management **73**:1333–1340.

Krebs, C. J. 1944. Ecology: the experimental analysis of distribution and abundance. HarperCollins College Publishers, New York.

Kulpa, S., E. Leger, E. Espeland, and E. Goergen. 2012. Postfire seeding and plant community recovery in the Great Basin. Rangeland Ecology & Management **65**:171–181.

Lauenroth, W., and O. E. Sala. 1992. Long-term forage production of North American shortgrass steppe. Ecological Applications **2**:397–403.

Little, R. J. 2006. Calibrated Bayes: a Bayes/frequentist roadmap. The American Statistician **60**:213–223.

Lockyer, Z. B., P. S. Coates, M. L. Casazza, S. Espinosa, and D. J. Delehanty. 2015. Nest-site selection and reproductive success of greater sage-grouse in a fire-affected habitat of northwestern Nevada. The Journal of Wildlife Management **79**:785–797.

Lu, X., P. J. Williams, M. B. Hooten, J. A. Powell, J. N. Womble, and M. R. Bower. 2020. Nonlinear reaction–diffusion process models improve inference for population dynamics. Environmetrics **31**:e2604.

Lyon, A. G., 2000. The potential effects of natural gas development on sage grouse near Pinedale, Wyoming. Ph.D. thesis, University of Wyoming.

Mahood, A. L., and J. K. Balch. 2019. Repeated fires reduce plant diversity in low-elevation Wyoming big sagebrush ecosystems (1984–2014). Ecosphere **10**:e02591.

McCaffery, R., J. J. Nowak, and P. M. Lukacs. 2016. Improved analysis of lek count data using N-mixture models. The Journal of Wildlife Management **80**:1011–1021.

Miller, R. F., S. T. Knick, D. A. Pyke, C. W. Meinke, S. E. Hanser, M. J. Wisdom, and A. L. Hild. 2011. Characteristics of sagebrush habitats and limitations to long-term conservation. Greater sage-grouse: ecology and conservation of a landscape species and its habitats. Studies in Avian Biology **38**:145–184.

Moynahan, B. J., M. S. Lindberg, and J. W. Thomas. 2006. Factors contributing to process variance in annual survival of female greater sage-grouse in Montana. Ecological Applications **16**:1529–1538.

Nevada Department of Wildlife, 2018. Nevada sage-grouse conservation project: final performance report. Technical Report FY2017, Nevada Department of Wildlife, 6980 Sierra Center Parkway, Suite 120, Reno, NV 89511.

Palmer, W. C. 1965. Meteorological drought. Research paper 45. Weather Bureau, Washington, DC .

Pandolfi, J. M., R. H. Bradbury, E. Sala, T. P. Hughes, K. A. Bjorndal, R. G. Cooke, D. McArdle, L. McClenachan, M. J. Newman, G. Paredes, et al. 2003. Global trajectories of the long-term decline of coral reef ecosystems. Science **301**:955–958.

Patterson, R. L. 1952. The sage grouse in Wyoming. Sage Books, Denver, Colorado, USA.

Peebles, L. W., M. R. Conover, and J. B. Dinkins. 2017. Adult sage-grouse numbers rise following raven removal or an increase in precipitation. Wildlife Society Bulletin **41**:471–478.

Petersen, B. E., 1980. Breeding and nesting ecology of female sage grouse in North Park, Colorado. Ph.D. thesis, Colorado State University.

Pratt, A. C., K. T. Smith, and J. L. Beck. 2017. Environmental cues used by greater sage-grouse to initiate altitudinal migration. The Auk: Ornithological Advances **134**:628–643.

R Core Team, 2019. R: A Language and Environment for Statistical Computing. R Foundation for Statistical Computing, Vienna, Austria. URL `https://www.R-project.org/`.

Renwick, K. M., C. Curtis, A. R. Kleinhesselink, D. Schlaepfer, B. A. Bradley, C. L. Aldridge, B. Poulter, and P. B. Adler. 2018. Multi-model comparison highlights consistency in predicted effect of warming on a semi-arid shrub. Global Change Biology **24**:424–438.

Rich, T., and B. Altman. 2002. Under the sage-grouse umbrella. Bird Conservation **14**:10.

Rich, T. D., M. J. Wisdom, and V. A. Saab, 2005. Conservation of priority birds in sagebrush ecosystems. Proceedings from the Third International Partners In Flight

Conference: A Workshop on Bird Conservation Implementation and Integration. Technical Report PSW-GTR-191, USDA Forest Service, Albany, California, USA.

Rigge, M., C. Homer, L. Cleeves, D. K. Meyer, B. Bunde, H. Shi, G. Xian, S. Schell, and M. Bobo. 2020. Quantifying Western US Rangelands as fractional components with multi-resolution remote sensing and in situ data. Remote Sensing **12**:412.

Row, J. R., and B. C. Fedy. 2017. Spatial and temporal variation in the range-wide cyclic dynamics of greater sage-grouse. Oecologia **185**:687–698.

Rowland, M. M., M. J. Wisdom, L. H. Suring, and C. W. Meinke. 2006. Greater sage-grouse as an umbrella species for sagebrush-associated vertebrates. Biological Conservation **129**:323–335.

Schroeder, M. A., J. R. Young, and C. E. Braun. 1999. Sage Grouse(Centrocercus urophasianus). The Birds of North America page 28.

Scott, J. W. 1942. Mating behavior of the sage grouse. The Auk **59**:477–498.

Sedinger, J. S. 2007. Improving understanding and assessment of greater sage-grouse populations. University of Idaho College of Natural Resources Experiment Station Bulletin **88**:43–56.

Slater, S. J., 2003. Sage-grouse (Centrocercus urophasianus) use of different-aged burns and the effects of coyote control in southwestern Wyoming. Ph.D. thesis, University of Wyoming.

Smith, J. T., J. D. Tack, L. I. Berkeley, M. Szczypinski, and D. E. Naugle. 2018. Effects of rotational grazing management on nesting greater sage-grouse. The Journal of Wildlife Management **82**:103–112.

Spiegelhalter, D. J., N. G. Best, B. P. Carlin, and A. Van Der Linde. 2002. Bayesian measures of model complexity and fit. Journal of the Royal Statistical Society: Series b (Statistical Methodology) **64**:583–639.

Street, P. A., 2020. Greater Sage-grouse habitat and demographic response to grazing by non-native ungulates. Ph.D. thesis, University of Nevada, Reno.

Suring, L. H., M. M. Rowland, and M. J. Wisdom, 2005. Identifying species of conservation concern, Pages 150–162 . Lawrence, Kan.: Alliance Communications Group, 2005.

Sveum, C. M., J. A. Crawford, and W. D. Edge. 1998. Use and selection of brood-rearing habitat by sage grouse in south central Washington. The Great Basin Naturalist pages 344–351.

US Fish and Wildlife Service, 2010. Endangered and threatened wildlife and plants; 12-month findings for petitions to list the greater sage-grouse (*Centrocercus urophasianus*) as threatened or endangered. Technical Report 55, Federal Register.

Walsh, D. P., G. C. White, T. E. Remington, and D. C. Bowden. 2004. Evaluation of the lek-count index for greater sage-grouse. Wildlife Society Bulletin **32**:56–68.

Wang, G. 2018. Bayesian spatiotemporal dynamic models for regional dynamics of avian populations. Ecological Informatics **45**:31–37.

Wenninger, E. J., and R. S. Inouye. 2008. Insect community response to plant diversity and productivity in a sagebrush–steppe ecosystem. Journal of Arid Environments **72**:24–33.

Western Association of Fish and Wildlife Agencies, 2015. Greater sage-grouse population trends: an analysis of lek count databases 1965–2015. Technical report, Western Association of Fish and Wildlife Agencies, Cheyenne, WY, USA.

Western Regional Climate Center, 2021. Climate of Nevada. URL `https://wrcc.dri.edu/Climate/narrative_nv.php`.

Wikle, C. K. 2003. Hierarchical Bayesian models for predicting the spread of ecological processes. Ecology **84**:1382–1394.

Wikle, C. K., and M. B. Hooten. 2010. A general science-based framework for dynamical spatio-temporal models. Test **19**:417–451.

Williams, P. J., M. B. Hooten, G. G. Esslinger, J. N. Womble, J. L. Bodkin, and M. R. Bower. 2019. The rise of an apex predator following deglaciation. Diversity and Distributions **25**:895–908.

Williams, P. J., M. B. Hooten, J. N. Womble, G. G. Esslinger, and M. R. Bower. 2018. Monitoring dynamic spatio-temporal ecological processes optimally. Ecology **99**:524–535.

Williams, P. J., M. B. Hooten, J. N. Womble, G. G. Esslinger, M. R. Bower, and T. J. Hefley. 2017. An integrated data model to estimate spatiotemporal occupancy, abundance, and colonization dynamics. Ecology **98**:328–336.

Wisdom, M. J., M. M. Rowland, L. H. Suring, D. S. Dobkin, and B. Abbey. 2005. Habitat Threats in the Sagebrush Ecosystem: Methods of Regional Assessment and Applications in the Great Basin. Allen Press, Lawrence, Kansas, USA.

5 Tables

Table 1: Covariates hypothesized to be correlated with expected lek counts in Nevada, from 2000–2018. Included is the covariate name, the abbreviation used in the main body of the text, the resolution or units used in the analysis, the direction of the hypothesized correlation, and other studies examining similar hypotheses.

Covariate	Abbreviation	Resolution/Units	Hypothesis Prediction	Citation
Elevation	elevation	30m	+	Farr et al. (2007)
Slope	slope	degrees	-	Jarvis et al. (2008)
Percent Bare Ground Cover	bare ground	30m	-	Rigge et al. (2020)
Percent Sagebrush Cover	sagebrush	30m	+	Rigge et al. (2020)
Water Bodies	water	30m	+	Feng et al. (2016)
Monthly Precipitation	ppt	mm	+	Gorelick et al. (2017); Daly et al. (2015)
Monthly Maximum Temperature	max temp	°C	-	Gorelick et al. (2017); Daly et al. (2015)
Fire Frequency	burn	500m	-	Giglio et al. (2015); Gorelick et al. (2017)
Normalized Difference Vegetation Index	NDVI	250m	+	Didan (2015); Gorelick et al. (2017)
Palmer Drought Severity Index	PDSI	2.5 arc minutes	+	Abatzoglou et al. (2018)

Table 2: Covariates I considered in each model I examined to predict expected lek attendance in Nevada, USA from 2000–2018. Descriptions of abbreviations are reported in Table 1.

ID	Covariates included in the model
Model 1	elevation+slope+bare ground+sagebrush+ppt+max temp+burn+NDVI+PDSI+water
Model 2	elevation+slope+bare ground+sagebrush+ppt+max temp+burn+NDVI+PDSI
Model 3	elevation+slope+bare ground+max temp+burn+PDSI
Model 4	ppt+max temp+burn+NDVI+PDSI
Model 5	elevation+sagebrush+ppt+NDVI
Model 6	elevation+slope+bare ground+sagebrush
Model 7	elevation+slope+ppt
Model 8	burn+PDSI
Model 9	sagebrush+ppt
Model 10	bare ground+burn

Table 3: Model selection results using Deviance Information Criterion (DIC) of each of the models I considered in the first-stage of model selection examining ability of each model to predict expected lek counts in Nevada, USA from 2000–2018. Model 2 had the lowest DIC score, suggesting it was the best predictive model in the model suite. Model descriptions are provided in Table 2.

ID	DIC	Δ DIC	Number of Parameters
Model 2	354003.7	0.0	9
Model 1	354961.2	957.5	10
Model 6	357098.4	3094.7	4
Model 3	357639.7	3636.0	6
Model 7	358975.9	4972.2	3
Model 4	361401.3	7397.6	5
Model 5	362674.6	8670.9	4
Model 10	363115.9	9112.2	2
Model 9	365725.9	11722.2	2
Model 8	367219.2	13215.5	2

Table 4: Median, 95% credible intervals, and mean of marginal posterior distributions for each parameter in Model 2, the best predictive model using the Deviance Information Criterion (DIC). Model 2 described in Table 2.

Parameter	2.5%	50%	97.5%	mean
β (Elevation)	0.277	0.293	0.308	0.293
β (Slope)	-0.362	-0.354	-0.345	-0.354
β (Bare Ground)	-0.108	-0.096	-0.085	-0.096
β (Sagebrush)	0.068	0.078	0.088	0.078
β (Precipitation)	-0.155	-0.146	-0.138	-0.146
β (Maximum Temperature)	-0.236	-0.224	-0.213	-0.224
β (Fire Frequency)	-0.015	-0.0045	0.0048	-0.0046
β (NDVI)	0.033	0.042	0.051	0.042
β (PDSI)	0.086	0.091	0.096	0.091
σ_α^2	3.83	5.18	7.26	5.27
ϕ (Range)	6063.03	6113.9	6319.3	6134.1

Table 5: Model selection results using Deviance Information Criterion (DIC) of each of the models I considered in the second-stage of model selection examining ability of each model to predict expected lek counts in Nevada, USA from 2008–2018. The 8-year precipitation lag had the lowest DIC score, suggesting it was the best predictive model in the model suite.

ID	DIC	Delta DIC	Number of Parameters
8-year Precip. Lag	240533.3	0	9
5-year Precip. Lag	240669	135.7	9
4-year Precip. Lag	240754.2	220.9	9
3-year Precip. Lag	240908.5	375.2	9
2-year Precip. Lag	241064.2	530.9	9
1-year Precip. Lag	241367.2	833.9	9
3-year PDSI Lag	241531.3	998	9
Model 2 Lag	241538	1004.7	9
4-year PDSI Lag	241539.3	1006	9
1-year PDSI Lag	241539.8	1006.5	9
2-year PDSI Lag	241542.1	1008.8	9
5-year PDSI Lag	241542.4	1009.1	9
8-year PDSI Lag	241546.9	1013.6	9
4-year Fire Lag	241552.9	1019.6	9
2-year Fire Lag	241555.3	1022	9
8-year Fire Lag	241561.2	1027.9	9
1-year Fire Lag	241562.4	1029.1	9

Table 6: Median, 95% credible intervals, and mean of marginal posterior distributions for each parameter in the 8-year precipitation mean model.

Parameter	2.5%	50%	97.5%	Mean
β (Elevation)	0.325	0.346	0.367	0.346
β (Slope)	-0.281	-0.270	-0.259	-0.270
β (Bare Ground)	-0.091	-0.075	-0.059	-0.075
β (Sagebrush)	0.024	0.037	0.049	0.037
β (Precipitation)	-0.299	-0.286	-0.272	-0.286
β (Maximum Temperature)	-0.339	-0.322	-0.304	-0.322
β (Fire Frequency)	-0.053	-0.036	-0.019	-0.035
β (NDVI)	0.008	0.066	0.082	0.066
β (PDSI)	0.097	0.106	0.114	0.106
σ_α^2	6.07	8.16	11.2	8.27
ϕ (Range)	6061.4	6076.8	6148.8	6084.2

6 Figures
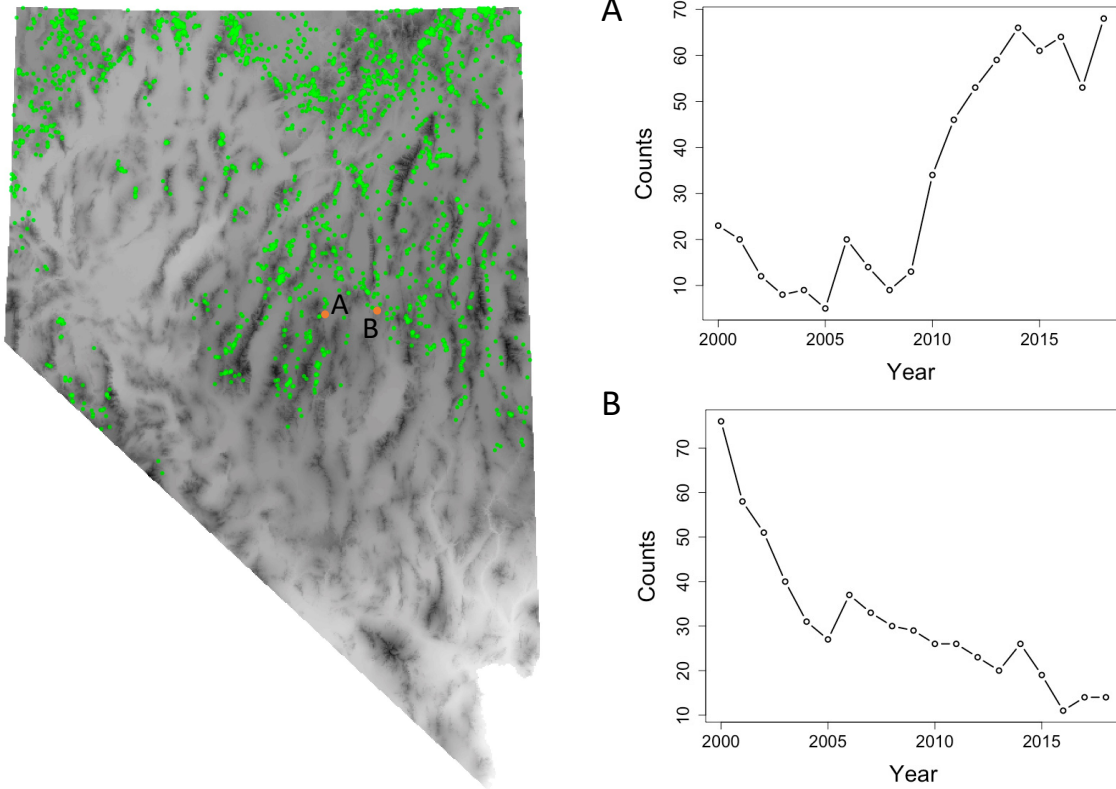
Figure 1: The GPS locations of 1,980 leks surveyed by the Nevada Department of Wildlife from 2000 to 2018, NV USA. Also shown are the counts from two leks in relative close proximity that experienced different trends from 2000–2018, suggesting that trends in lek counts vary substantially over space and time.
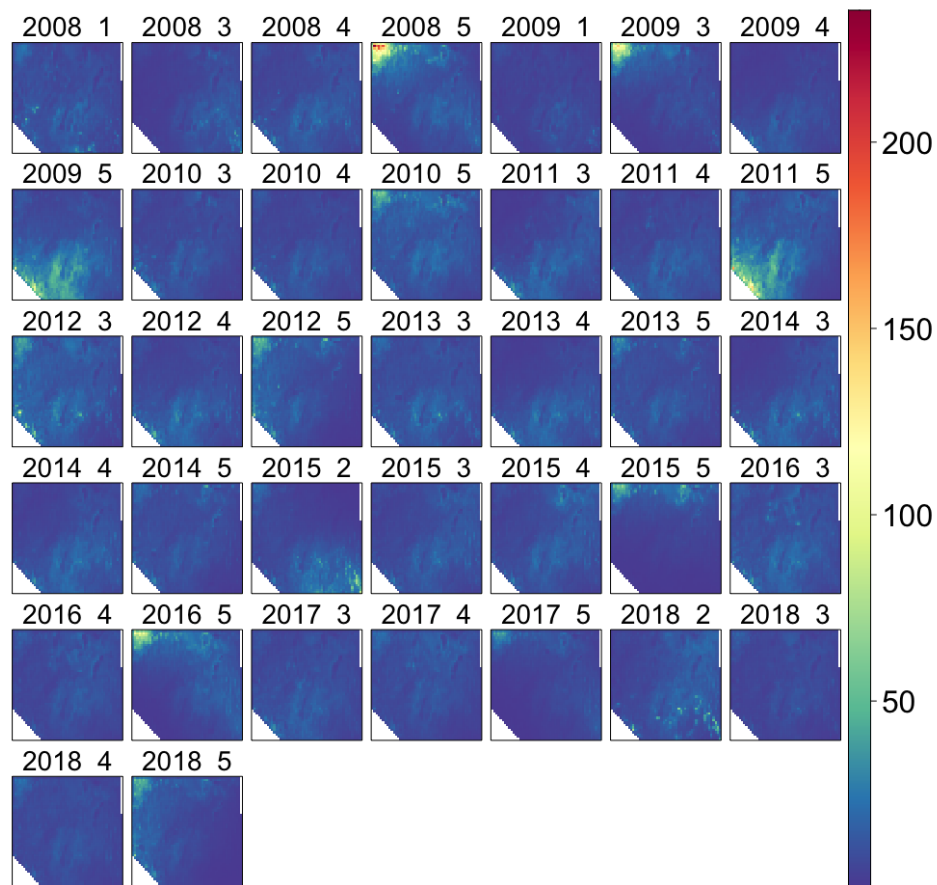
Figure 2: The change in expected lek counts through space and time using the top model (8-year precipitation lag) for Nevada, USA, for each of the 37 months of lek count data from 2008-2018. Units are the expected lek counts at a lek.
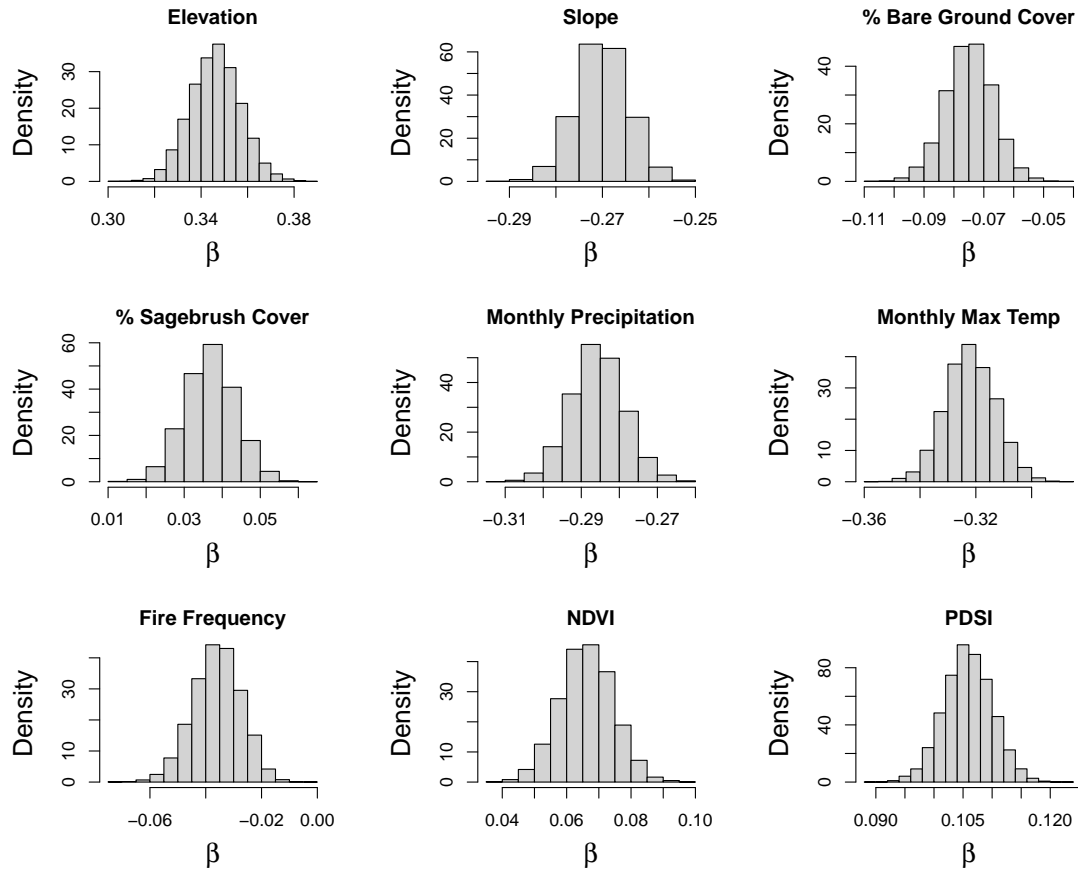
Figure 3: Estimated marginal posterior distributions for β from from the eight-year precipitation lag effects model.
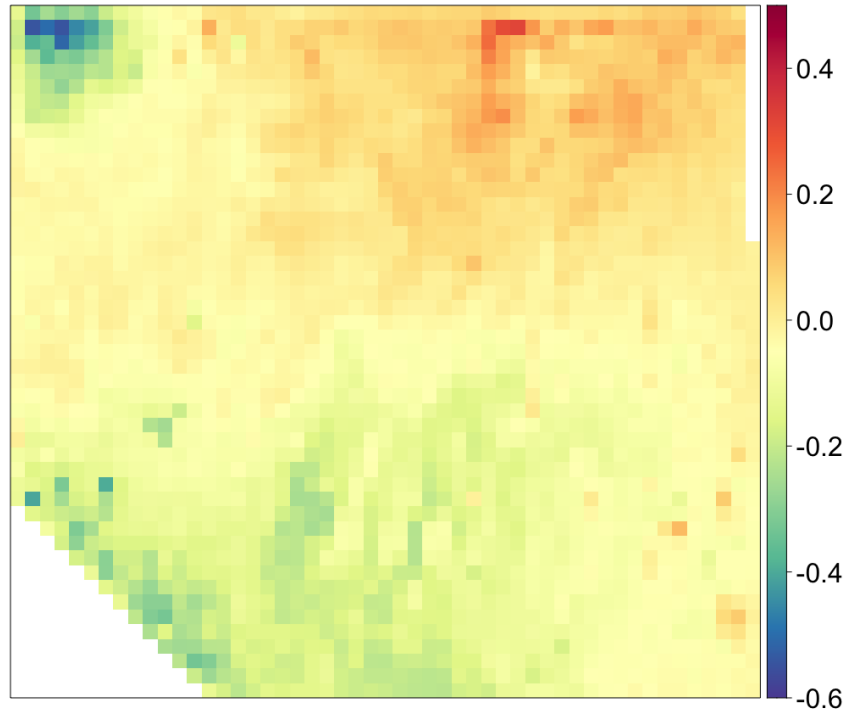
Figure 4: Population mean trend in expected lek counts from 2008-2018. Values equal to 0 have no change in expected lek counts. Positive values represent a positive trend, and negative values represent a negative trend. Expected lek counts appeared to decline everywhere in Nevada, USA except for the northeastern part of the state and other isolated populations across the state.
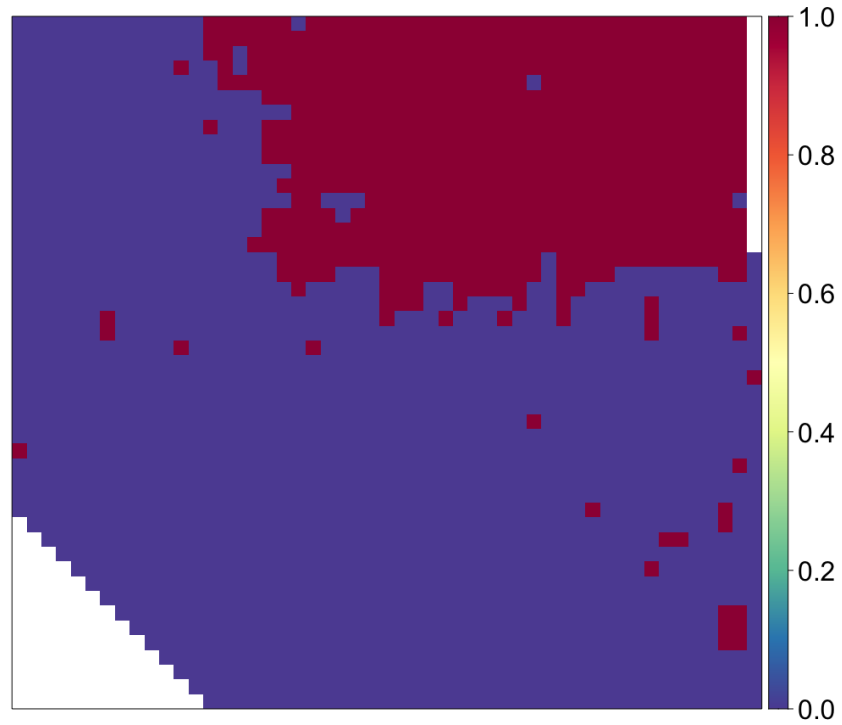
Figure 5: Map discretizing the continuous values from Figure 4 into either positive (i.e., $E([\gamma_1|\mathbf{y}]) > 0$; red) or negative (i.e., $E([\gamma_1|\mathbf{y}]) < 0$; blue) to identify where populations have increased or decreased on average in Nevada from 2008–2018.
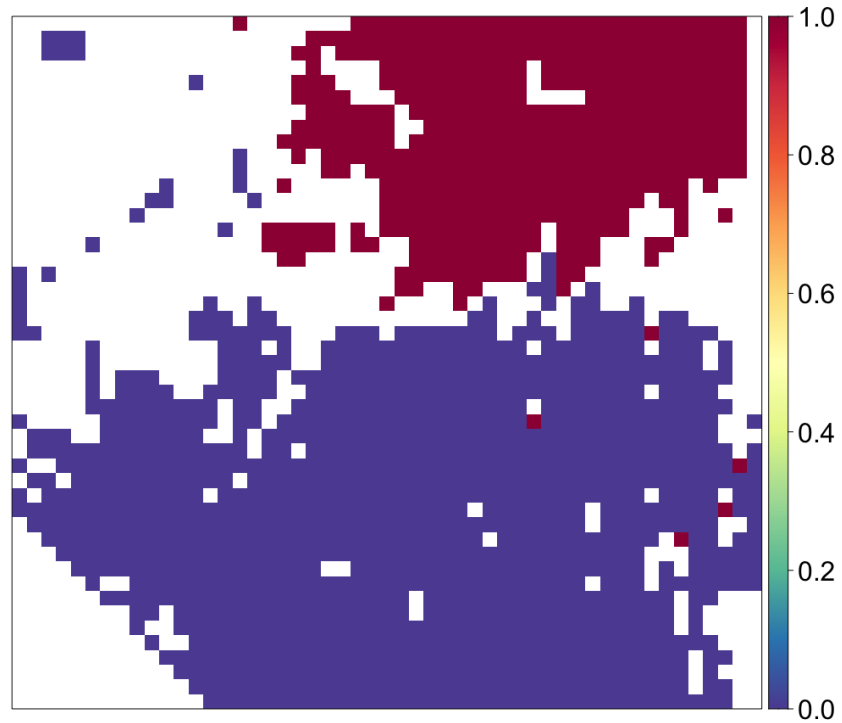
Figure 6: Characterization of the uncertainty in trend estimates in Nevada from 2008–2018. Values of 1 (red) indicate positive trend and 95% credible intervals that did not overlap zero, values of 0 (blue) indicate negative trend and 95% credible intervals that did not overlap zero. White represents areas where the 95% credible intervals overlapped zero.
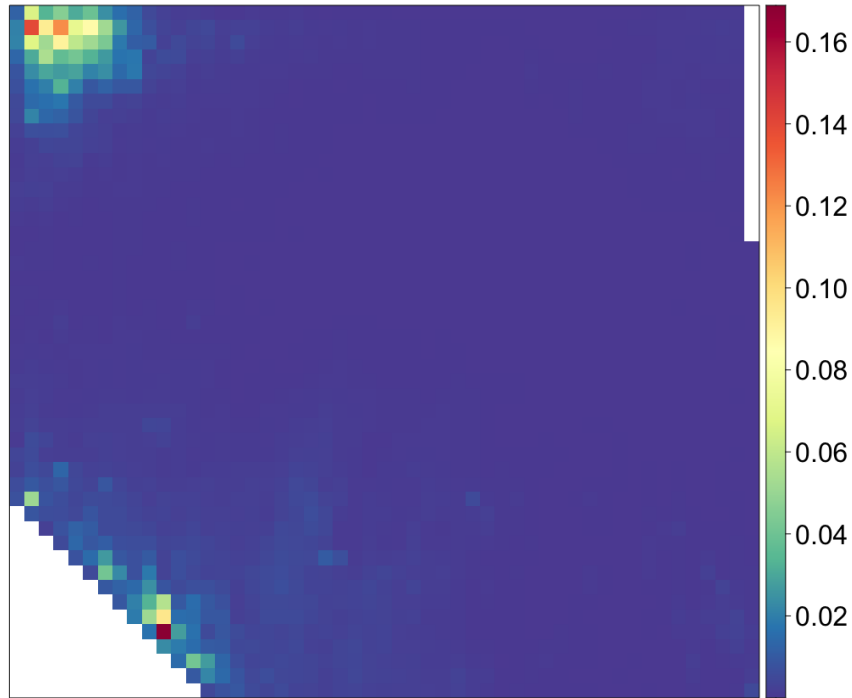
Figure 7: Variance in the 95% credible interval of the posterior distribution of trend estimate (γ_1) of sage grouse expected lek counts from 2008–2018 in Nevada, USA. Variance was calculated using $\frac{\sum_{k=1}^{K}(\gamma_1^{(k)} - \frac{1}{K}\sum_{k=1}^{K}\gamma_1^{(k)})^2}{K-1}$ for $k = 1, ..., K$ MCMC iterations. Two areas with the most variability in the trend estimates included the Bi-State population and the population near the Sheldon National Wildlife Refuge. Despite the variability in these areas, some locations had 95% CRIs that did not overlap 0, suggesting the populations were declining, but there is uncertainty in the rate of decline.
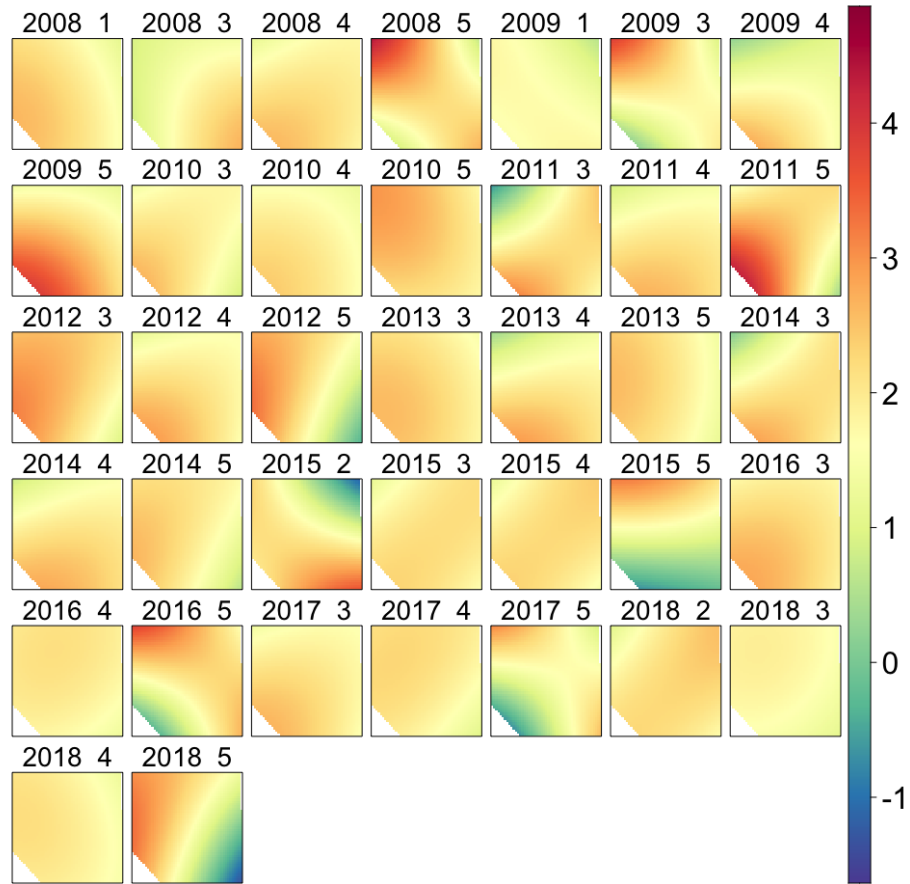
Figure 8: The spatial random effect, $\boldsymbol{\Phi\alpha}_t$, for each time period $t = 1, \ldots, 37$ used to address spatial autocorrelation in expected lek counts, conditional on $\boldsymbol{X\beta}_t$. Red areas indicate expected lek counts were higher than predicted by $\boldsymbol{X\beta}_t$, and blue areas indicate expected lek counts were lower than predicted by $\boldsymbol{X\beta}_t$.
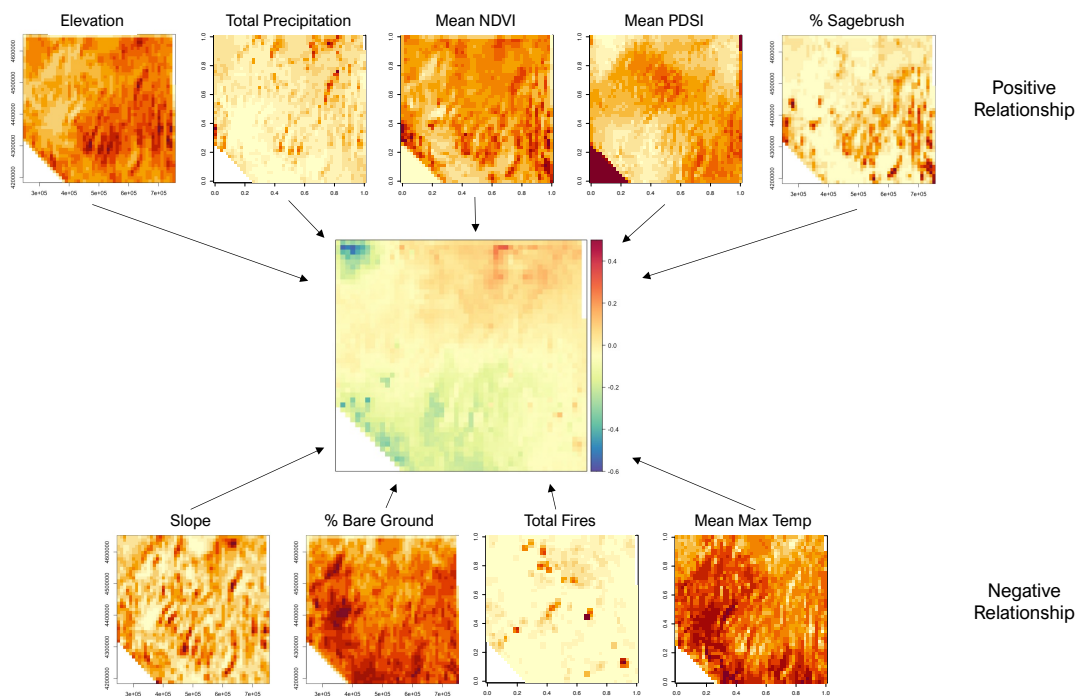
Figure 9: Mean trend in expected lek counts (center) and the mean of each covariate in the top model from 2008-2018 depicting exogenous drivers in space and their relationship (positive or negative) to sage grouse populations after addressing spatio-temporal autocorrelation.
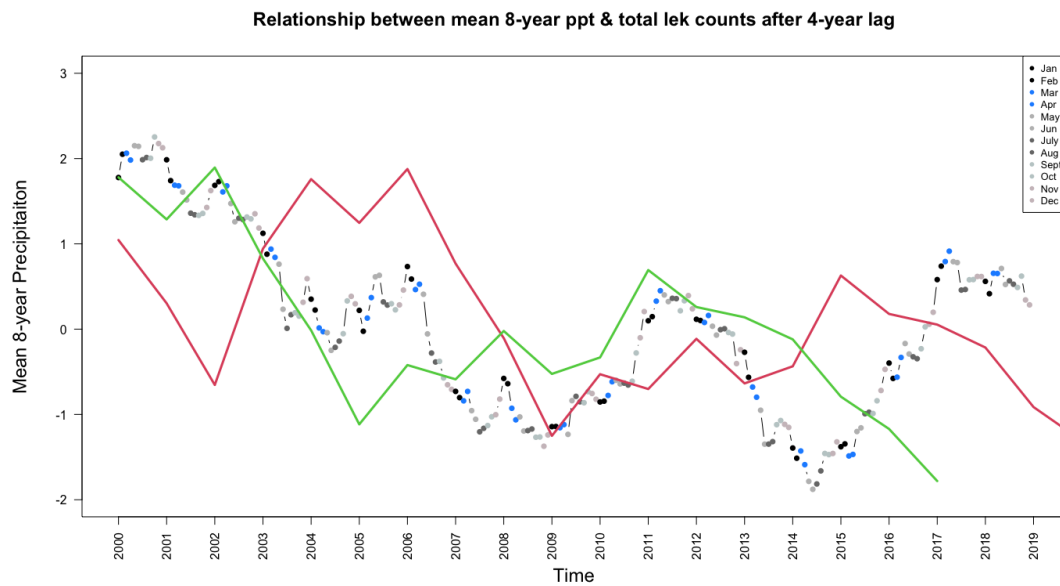
Figure 10: The 8-year precipitation mean from 2000-2018 (dotted line), expected lek counts across Nevada (red line), and expected lek counts shifted left 4 years (green line) to portray the relationship between 8-year precipitation mean and total lek counts after a 4-year lag period (green).

7 Appendices

Appendix A

Table 7: Number of Sage grouse counted per month from 2000-2018

Month.ID	Month	Year	Total Sage Grouse Counted
1	1	2000	4498
2	2	2000	0
3	3	2000	19
4	4	2000	39
5	5	2000	5
6	6	2000	0
7	7	2000	0
8	8	2000	0
9	9	2000	0
10	10	2000	0
11	11	2000	0
12	12	2000	0
13	1	2001	4462
14	2	2001	0
15	3	2001	35

Table 7: Number of Sage grouse counted per month from 2000-2018 *(continued)*

Month.ID	Month	Year	Total Sage Grouse Counted
16	4	2001	115
17	5	2001	12
18	6	2001	0
19	7	2001	0
20	8	2001	0
21	9	2001	0
22	10	2001	0
23	11	2001	0
24	12	2001	0
25	1	2002	4802
26	2	2002	0
27	3	2002	129
28	4	2002	145
29	5	2002	6
30	6	2002	0
31	7	2002	0
32	8	2002	0
33	9	2002	0
34	10	2002	0

Table 7: Number of Sage grouse counted per month from 2000-2018 *(continued)*

Month.ID	Month	Year	Total Sage Grouse Counted
35	11	2002	0
36	12	2002	0
37	1	2003	4829
38	2	2003	0
39	3	2003	75
40	4	2003	120
41	5	2003	0
42	6	2003	0
43	7	2003	0
44	8	2003	0
45	9	2003	0
46	10	2003	0
47	11	2003	0
48	12	2003	0
49	1	2004	7231
50	2	2004	0
51	3	2004	123
52	4	2004	77
53	5	2004	52

Table 7: Number of Sage grouse counted per month from 2000-2018 *(continued)*

Month.ID	Month	Year	Total Sage Grouse Counted
54	6	2004	0
55	7	2004	0
56	8	2004	0
57	9	2004	0
58	10	2004	0
59	11	2004	0
60	12	2004	0
61	1	2005	9456
62	2	2005	0
63	3	2005	412
64	4	2005	347
65	5	2005	56
66	6	2005	0
67	7	2005	0
68	8	2005	0
69	9	2005	0
70	10	2005	0
71	11	2005	0
72	12	2005	0

Table 7: Number of Sage grouse counted per month from 2000-2018 *(continued)*

Month.ID	Month	Year	Total Sage Grouse Counted
73	1	2006	6626
74	2	2006	0
75	3	2006	1189
76	4	2006	2954
77	5	2006	639
78	6	2006	0
79	7	2006	0
80	8	2006	0
81	9	2006	0
82	10	2006	0
83	11	2006	0
84	12	2006	0
85	1	2007	9640
86	2	2007	0
87	3	2007	912
88	4	2007	842
89	5	2007	74
90	6	2007	0
91	7	2007	0

Table 7: Number of Sage grouse counted per month from 2000-2018 *(continued)*

Month.ID	Month	Year	Total Sage Grouse Counted
92	8	2007	0
93	9	2007	0
94	10	2007	0
95	11	2007	0
96	12	2007	0
97	1	2008	5325
98	2	2008	0
99	3	2008	293
100	4	2008	1277
101	5	2008	670
102	6	2008	0
103	7	2008	0
104	8	2008	0
105	9	2008	0
106	10	2008	0
107	11	2008	0
108	12	2008	0
109	1	2009	1422
110	2	2009	40

Table 7: Number of Sage grouse counted per month from 2000-2018 *(continued)*

Month.ID	Month	Year	Total Sage Grouse Counted
111	3	2009	1023
112	4	2009	2440
113	5	2009	581
114	6	2009	0
115	7	2009	0
116	8	2009	0
117	9	2009	0
118	10	2009	0
119	11	2009	0
120	12	2009	0
121	1	2010	44
122	2	2010	0
123	3	2010	1491
124	4	2010	5059
125	5	2010	2125
126	6	2010	0
127	7	2010	0
128	8	2010	0
129	9	2010	0

Table 7: Number of Sage grouse counted per month from 2000-2018 *(continued)*

Month.ID	Month	Year	Total Sage Grouse Counted
130	10	2010	0
131	11	2010	0
132	12	2010	0
133	1	2011	0
134	2	2011	38
135	3	2011	1560
136	4	2011	5163
137	5	2011	2047
138	6	2011	14
139	7	2011	0
140	8	2011	0
141	9	2011	0
142	10	2011	0
143	11	2011	0
144	12	2011	0
145	1	2012	2
146	2	2012	12
147	3	2012	2745
148	4	2012	7517

Table 7: Number of Sage grouse counted per month from 2000-2018 *(continued)*

Month.ID	Month	Year	Total Sage Grouse Counted
149	5	2012	1849
150	6	2012	0
151	7	2012	0
152	8	2012	0
153	9	2012	0
154	10	2012	0
155	11	2012	0
156	12	2012	0
157	1	2013	0
158	2	2013	0
159	3	2013	2648
160	4	2013	5369
161	5	2013	1262
162	6	2013	0
163	7	2013	0
164	8	2013	0
165	9	2013	0
166	10	2013	0
167	11	2013	0

Table 7: Number of Sage grouse counted per month from 2000-2018 *(continued)*

Month.ID	Month	Year	Total Sage Grouse Counted
168	12	2013	0
169	1	2014	0
170	2	2014	49
171	3	2014	4214
172	4	2014	6204
173	5	2014	1411
174	6	2014	42
175	7	2014	0
176	8	2014	0
177	9	2014	0
178	10	2014	0
179	11	2014	0
180	12	2014	0
181	1	2015	0
182	2	2015	237
183	3	2015	6835
184	4	2015	8106
185	5	2015	694
186	6	2015	1

Table 7: Number of Sage grouse counted per month from 2000-2018 *(continued)*

Month.ID	Month	Year	Total Sage Grouse Counted
187	7	2015	0
188	8	2015	0
189	9	2015	0
190	10	2015	0
191	11	2015	0
192	12	2015	0
193	1	2016	0
194	2	2016	0
195	3	2016	4999
196	4	2016	7937
197	5	2016	1943
198	6	2016	0
199	7	2016	0
200	8	2016	0
201	9	2016	0
202	10	2016	0
203	11	2016	0
204	12	2016	0
205	1	2017	0

Table 7: Number of Sage grouse counted per month from 2000-2018 *(continued)*

Month.ID	Month	Year	Total Sage Grouse Counted
206	2	2017	36
207	3	2017	4042
208	4	2017	6741
209	5	2017	2073
210	6	2017	0
211	7	2017	0
212	8	2017	0
213	9	2017	0
214	10	2017	0
215	11	2017	0
216	12	2017	0
217	1	2018	0
218	2	2018	134
219	3	2018	4857
220	4	2018	6074
221	5	2018	997
222	6	2018	0
223	7	2018	0
224	8	2018	0

Table 7: Number of Sage grouse counted per month from 2000-2018 *(continued)*

Month.ID	Month	Year	Total Sage Grouse Counted
225	9	2018	0
226	10	2018	0
227	11	2018	0
228	12	2018	0

Appendix B
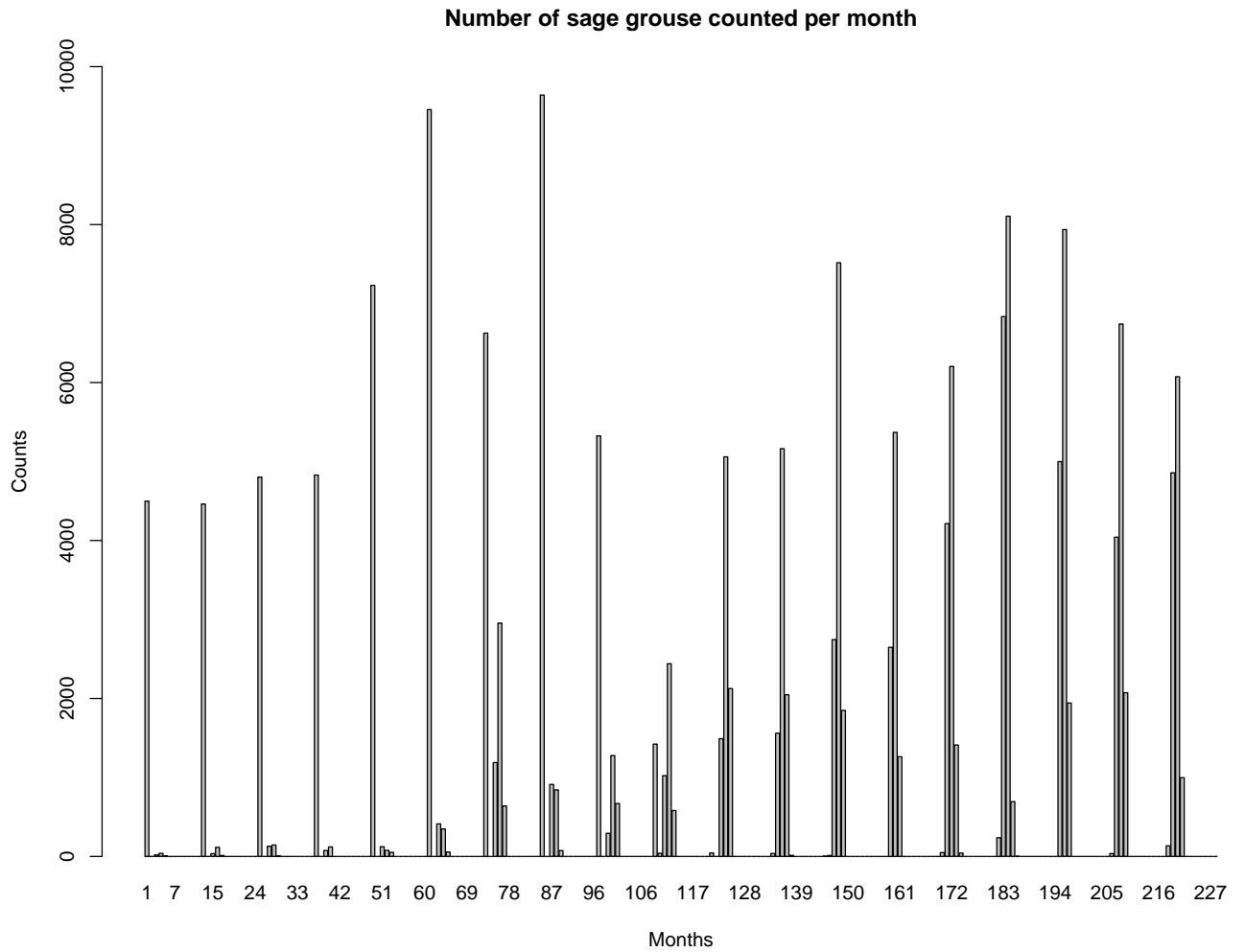
Figure 11: The total number of sage grouse counted per month from 2000 to 2018.

Appendix C

```
##################################################################
###
### Spatial Temporal Script - 8-year Precipitation Lag
###
##################################################################



rm( list=ls ())
## set.seed(2021)


real.data=TRUE
pre.tuned=TRUE


###
### Libraries
###


library(coda)
library(fields)
library(gridExtra)
library(MASS)
library(Matrix)
library(mgcv)
library(mvtnorm)
library(raster)
library(rgdal)
library(rasterVis)
library(RColorBrewer)
library(RSpectra)
library(truncnorm)
library(dplyr)
library(beepr)


################################################################
#### Simulated Data Analysis
################################################################


###
### Set working directory
###
```

```
setwd("~/Dropbox/SageGrouseProject")


###
### x and y bounds
###


ymn=4181000
ymx=4653000
xmn=246000
xmx=756000


###
### Resolution
###


res=10000


###
### Create an empty raster
###


r=raster(,xmn=xmn,xmx=xmx,ymn=ymn,ymx=ymx,resolution=res)


###
### Domain
###


nx=ncol(r)
ny=nrow(r)
q=nx*ny
x.v=1:nx
y.v=1:ny


###
### Months with >100 observations
###


months.ind=c( 97L,  99L,  100L,  101L,
              109L,  111L,  112L,  113L,  123L,  124L,  125L,  135L,  136L,  137L,
              147L,  148L,  149L,  159L,  160L,  161L,  171L,  172L,  173L,  182L,
              183L,  184L,  185L,  195L,  196L,  197L,  207L,  208L,  209L,  218L,
              219L,  220L,  221L
)


###
```

```r
### Number of time periods , basis functions , and time differences
###

T=length(months.ind)
n=1980 # max number of leks
n.a=4 #basis functions
t.dif=months.ind[-1]-months.ind[-length(months.ind)]


###
### Distance
###

coords=expand.grid(x.v,rev(y.v))
D=as.matrix(dist(coords,diag=TRUE,upper=TRUE))


###
### Coordinate reference system of all the spatial data
###

crs(r)=paste0("+proj=utm +zone=11 +datum=NAD83 +units=m",
              " +no_defs +ellps=GRS80 +towgs84=0,0,0 ")


#################################################################
### Load Data
#################################################################

df=read.csv("lekdata_for_model.csv")
df=df[order(df$easting,df$northing),]
df <- df[!(df$lekid == "DES-057"),]


load("Covariates28.RData")

boundary=elev
boundary[boundary<600]=NA
boundary[boundary>=600]=1


###
### Covariate matrix
###

X.l = list()
j=1
for(t in months.ind){
  X.l[[j]] = cbind(scale(elev[]),
                   scale(slope[]),
```

```
                        scale(bare[]),
                        scale(sage[]),
                        scale(pptlag8yr[[t]][]),
                        scale(tmax[[t]][]),
                        scale(burn[[t]][]),
                        scale(ndvi[[t]][]),
                        scale(pdsi[[t]][])
    )
    X.l[[j]][is.na(X.l[[j]])] <- 0
    j=j+1
}
X.m=rbind(X.l[[1]],X.l[[2]])
for(k in 3:length(months.ind)){
    X.m = rbind(X.m,X.l[[k]])
}
X.m[,ncol(X.l[[1]])-1]=scale(X.m[,ncol(X.l[[1]])-1])
X.m[,ncol(X.l[[1]])]=X.m[,ncol(X.l[[1]])-1]^2


###
### Cell ID
###


cell=r
cell[]=1:length(cell)
################################################################
### Incidence matrix
################################################################


H=list()
j=1
for(t in months.ind){
    df.tmp=subset(df,time==t)
    df.tmp=df.tmp[order(df.tmp$id),]
    cell.id=raster::extract(cell,cbind(df.tmp$easting,df.tmp$northing))
    H[[j]]=matrix(0,n,length(cell))
    for(i in 1:n){
        cell.id.tmp=cell.id[i]
        if(!is.na(df.tmp$y[i])){
            H[[j]][i,cell.id.tmp]=1
        }
    }
    j=j+1
}


###
```

```
### Block diagonal incidence matrix for all times to avoid a list with
### one matrix for each season, year combination.
###

H.bd=bdiag(H[[1]])
for(i in 2:length(H)){
  H.bd=bdiag(H.bd,H[[i]])
}


Y.tmp=subset(df,time==months.ind[1])
Y=Y.tmp[order(Y.tmp$id),11]

months.ind.2 = months.ind[-1]
for(t in months.ind.2){
  Y.tmp=subset(df,time==t)
  Y=c(Y,Y.tmp[order(Y.tmp$id),11])
}
Y=matrix(Y,length(Y),1)

###
###
###

y.s=seq(1,n*T,n)
y.e=seq(n,n*T,n)
ls=seq(1,q*T,q)
le=seq(q,q*T,q)

i=1
t=1
counts.per.month=0
for(t in 1:T){
  counts.per.month[t]=sum(Y[y.s[t]:y.e[t],], na.rm = TRUE)
}

###
### Simulated data
###

if(!real.data){
  phi.truth=9000
  phi=phi.truth
  R=exp(-D^2/phi)
  E=eigs_sym(R,n.a,which="LM")
```

```r
Phi=E$vectors%*%diag(E$values^(1/2))
s2.alpha.truth=matrix(c(0.001,0.001*t.dif),n.a,T,byrow=TRUE)
beta.truth=rnorm(ncol(X.m),0,.1)
alpha.truth=matrix(NA,n.a,T)
alpha.truth[,1]=c(-1,2,-3,1)
lambda.truth=matrix(NA,t*q,1)
lambda.truth[ls[1]:le[1]]=exp(c(Phi%*%alpha.truth[,1])+
                                X.m[ls[1]:le[1],]%*%beta.truth)
Y[y.s[1]:y.e[1]]=rpois(n,as.matrix(H.bd[y.s[1]:y.e[1],
                                ls[1]:le[1]]%*%
                                lambda.truth[ls[1]:le[1]]))
for(t in 2:T){
  alpha.truth[,t]=rnorm(n.a,alpha.truth[,t-1],sqrt(s2.alpha.truth[,t]))
  lambda.truth[ls[t]:le[t]]=exp(c(Phi%*%alpha.truth[,t])+
                                X.m[ls[t]:le[t],]%*%beta.truth)
  Y[y.s[t]:y.e[t]]=rpois(n,as.matrix(H.bd[y.s[t]:y.e[t],
                                ls[t]:le[t]]%*%
                                lambda.truth[ls[t]:le[t]]))
}
}


################################################################
###
################################################################


###
### MCMC settings
###

n.iter=300000


###
### Priors
###

phi.prior=c(0,500000)
alpha.prior=c(0,100)
s2.alpha.prior=c(0,20)
beta.prior=c(0,1)


###
### Starting values
###

phi=9000
```

```
R=exp(-D^2/phi)

E=eigs_sym(R,n.a,which="LM")

Phi=E$vectors%*%diag(E$values^(1/2))

s2.alpha=matrix(c(0.001,0.001*t.dif),n.a,T,byrow=TRUE)

beta=rnorm(ncol(X.m),0,.1)

alpha=matrix(NA,n.a,T)

alpha[,1]=c(-1,2,-3,1)

lambda=matrix(NA,t*q,1)

lambda[ls[1]:le[1]]=exp(c(Phi%*%alpha[,1])+
                          X.m[ls[1]:le[1],]%*%beta)

for(t in 2:T){

  alpha[,t]=rnorm(n.a,alpha[,t-1],sqrt(s2.alpha[,t]))

  lambda[ls[t]:le[t]]=exp(c(Phi%*%alpha[,t])+
                           X.m[ls[t]:le[t],]%*%beta)

}


if(!real.data){

  phi=phi.truth

  R=exp(-D^2/phi)

  E=eigs_sym(R,n.a,which="LM")

  Phi=E$vectors%*%diag(E$values^(1/2))

  beta=beta.truth#rnorm(length(beta.truth))

  alpha=alpha.truth

  lambda=lambda.truth## matrix(NA,T*q,1)

  ## for(t in 1:T){

  ##      #alpha[,t]=rnorm(n.a,alpha[,t-1],sqrt(s2.alpha[,t]))

  ##      lambda[ls[t]:le[t]]=exp(c(Phi%*%alpha[,t])+

  ##                              X.m[ls[t]:le[t],]%*%beta)

  ## }

  s2.alpha=s2.alpha.truth


}



###

### Tuning parameters

###


phi.tune=118.8065

alpha.tune=rep(0.01,T)

s2.alpha.tune=7.17101e-10

beta.tune=rep(0.001774625,length(beta))


if(pre.tuned){

  load("~/Dropbox/SageGrouseProject/PrecipitationLag_Tuners4.RData")
```

```r
    phi.tune=samples$phi.tune
    alpha.tune=samples$alpha.tune
    s2.alpha.tune=samples$s2.alpha.tune
    beta.tune=samples$beta.tune
}


###
### Bookkeeping
###

phi.save=matrix(NA,n.iter,1)
accept.phi=0
alpha.save=matrix(NA,n.iter,n.a*T)
accept.alpha=rep(0,T)
s2.alpha.save=matrix(NA,n.iter,T)
accept.s2.alpha=0
beta.save=matrix(NA,n.iter,ncol(X.m))
accept.beta=rep(0,length(beta))



DIC.save = numeric(1)
pd2.save = numeric(1)
Davg.save=rep(NA,n.iter)


################################################################
### Begin Gibbs loop
################################################################

system.time(
  for(k in 1:n.iter){
    if(k%%100==0)cat( k,"_")


    ##
    ## phi (MH)
    ##

    phi.star=rnorm(1,phi,phi.tune)
    if(phi.star>phi.prior[1]&phi.star<phi.prior[2]){
      R.star=exp(-D^2/phi.star)
      E.star=eigs_sym(R.star,n.a,which="LM")
      Phi.star=E.star$vectors%*%diag(E.star$values^(1/2),
                                  nrow=n.a,ncol=n.a)
      lambda.star=exp(c(Phi.star%*%alpha)+X.m%*%beta)
      mh1=sum(dpois(Y,as.matrix(H.bd%*%lambda.star),log=TRUE),
              na.rm = TRUE)
```

```
mh2=sum(dpois(Y,as.matrix(H.bd%*%lambda),log=TRUE),
         na.rm = TRUE)
mh=exp(mh1-mh2)
if(mh>runif(1)){
   phi=phi.star
   R=R.star
   E=E.star
   Phi=Phi.star
   lambda=lambda.star
   accept.phi=accept.phi+1
}
}


##
## alpha 1
##


alpha.star=rnorm(n.a,
                 alpha[,1],
                 alpha.tune[1])
lambda.star=exp(Phi%*%alpha.star+X.m[ls[1]:le[1],]%*%beta)


mh1=sum(dpois(Y[y.s[1]:y.e[1]],
              as.matrix(H.bd[y.s[1]:y.e[1],
                              ls[1]:le[1]]%*%lambda.star),
              log=TRUE),na.rm=TRUE)+
  sum(dnorm(alpha.star,alpha.prior[1],
            alpha.prior[2],
            log=TRUE))+
  sum(dnorm(alpha[,2],alpha.star,
            sqrt(s2.alpha[,2]),
            log=TRUE))
mh2=sum(dpois(Y[y.s[1]:y.e[1]],
              as.matrix(H.bd[y.s[1]:y.e[1],
                              ls[1]:le[1]]%*%lambda[ls[1]:le[1]]),
              log=TRUE),na.rm=TRUE)+
  sum(dnorm(alpha[,1],alpha.prior[1],
            alpha.prior[2],
            log=TRUE))+
  sum(dnorm(alpha[,2],alpha[,1],
            sqrt(s2.alpha[,2]),
            log=TRUE))
mh=exp(mh1-mh2)
if(mh>runif(1)){
   alpha[,1]=alpha.star
```

```r
    lambda[ls[1]:le[1],1]=lambda.star
    accept.alpha[1]=accept.alpha[1]+1
}


##
## alpha 2,...T-1
##

for(t in 2:(T-1)){
  alpha.star=rnorm(n.a,
                   alpha[,t],
                   alpha.tune[t])
  lambda.star=exp(Phi%*%alpha.star+X.m[ls[t]:le[t],]%*%beta)


  mh1=sum(dpois(Y[y.s[t]:y.e[t]],
                as.matrix(H.bd[y.s[t]:y.e[t],
                               ls[t]:le[t]]%*%lambda.star),
                log=TRUE),na.rm=TRUE)+
    sum(dnorm(alpha.star,alpha[,t-1],
              sqrt(s2.alpha[,t]),
              log=TRUE))+
    sum(dnorm(alpha[,t+1],alpha.star,
              sqrt(s2.alpha[,t+1]),
              log=TRUE))
  mh2=sum(dpois(Y[y.s[t]:y.e[t]],
                as.matrix(H.bd[y.s[t]:y.e[t],
                               ls[t]:le[t]]%*%lambda[ls[t]:le[t]]),
                log=TRUE),na.rm=TRUE)+
    sum(dnorm(alpha[,t],alpha[,t-1],
              sqrt(s2.alpha[,t]),
              log=TRUE))+
    sum(dnorm(alpha[,t+1],alpha[,t],
              sqrt(s2.alpha[,t+1]),
              log=TRUE))
  mh=exp(mh1-mh2)
  if(mh>runif(1)){
    alpha[,t]=alpha.star
    lambda[ls[t]:le[t],1]=lambda.star
    accept.alpha[t]=accept.alpha[t]+1
  }
}


alpha.star=rnorm(n.a,
                 alpha[,T],
                 alpha.tune[T])
```

```r
lambda.star=exp(Phi%*%alpha.star+X.m[ls[T]:le[T],]%*%beta)


mh1=sum(dpois(Y[y.s[T]:y.e[T]],
              as.matrix(H.bd[y.s[T]:y.e[T],
                            ls[T]:le[T]]%*%lambda.star),
              log=TRUE),na.rm=TRUE)+
  sum(dnorm(alpha.star,alpha[,T-1],
            sqrt(s2.alpha[,T]),
            log=TRUE))
mh2=sum(dpois(Y[y.s[T]:y.e[T]],
              as.matrix(H.bd[y.s[T]:y.e[T],
                            ls[T]:le[T]]%*%lambda[ls[T]:le[T]]),
              log=TRUE),na.rm=TRUE)+
  sum(dnorm(alpha[,T],alpha[,T-1],
            sqrt(s2.alpha[,T]),
            log=TRUE))
mh=exp(mh1-mh2)
if(mh>runif(1)){
  alpha[,T]=alpha.star
  lambda[ls[T]:le[T],1]=lambda.star
  accept.alpha[T]=accept.alpha[T]+1
}


##
## s2.alpha
##


s2.alpha.star.tmp=rtruncnorm(1,a=s2.alpha.prior[1],b=s2.alpha.prior[2],
                             mean=s2.alpha[1],sd=sqrt(s2.alpha.tune))
s2.alpha.star=matrix(c(s2.alpha.star.tmp,s2.alpha.star.tmp*t.dif),n.a,T,byrow=TRUE)


mh1=sum(dnorm(alpha[,-1],alpha[,-T],sqrt(s2.alpha.star[,-1]),
              log=TRUE))+
  log(dtruncnorm(s2.alpha[1],a=s2.alpha.prior[1],b=s2.alpha.prior[2],
                 mean=s2.alpha.star.tmp,sd=sqrt(s2.alpha.tune)))
mh2=sum(dnorm(alpha[,-1],alpha[,-T],sqrt(s2.alpha[,-1]),
              log=TRUE))+
  log(dtruncnorm(s2.alpha.star.tmp,a=s2.alpha.prior[1],b=s2.alpha.prior[2],
                 mean=s2.alpha[1],sd=sqrt(s2.alpha.tune[1])))


mh=exp(mh1-mh2)
if(mh>runif(1)){
  s2.alpha=s2.alpha.star
  accept.s2.alpha=accept.s2.alpha+1
}
```

```r
##
## beta
##

for(i in 1:length(beta)){
  beta.star=beta
  beta.star[i]=rnorm(1,beta[i],beta.tune[i])
  lambda.star=exp(c(Phi%*%alpha)+X.nf%*%beta.star)
  mh1=sum(dpois(Y,
                as.matrix(H.bd%*%lambda.star),log=TRUE),
          na.rm = TRUE)+
    sum(dnorm(beta.star[i],beta.prior[1],beta.prior[2],log=TRUE))
  mh2=sum(dpois(Y,
                as.matrix(H.bd%*%lambda),log=TRUE),
          na.rm = TRUE)+
    sum(dnorm(beta[i],beta.prior[1],beta.prior[2],log=TRUE))
  mh=min(exp(mh1-mh2),1)
  if(mh>runif(1)){
    beta=beta.star
    lambda=lambda.star
    accept.beta[i]=accept.beta[i]+1
  }
}


##
## Autotune
##

if(accept.phi/k>0.5) phi.tune=phi.tune*1.1
if(accept.phi/k<0.3) phi.tune=phi.tune*0.9


alpha.tune=ifelse(accept.alpha/k>0.5,alpha.tune*1.1,
                  ifelse(accept.alpha/k<0.3,alpha.tune*0.9,
                         alpha.tune)
)


if(accept.s2.alpha/k>0.5) s2.alpha.tune=s2.alpha.tune*1.1
if(accept.s2.alpha/k<0.3) s2.alpha.tune=s2.alpha.tune*0.9
## if(accept.beta/k>0.5) beta.tune=beta.tune*1.1
## if(accept.beta/k<0.3) beta.tune=beta.tune*0.9
beta.tune=ifelse(accept.beta/k>0.5,beta.tune*1.1,
                 ifelse(accept.beta/k<0.3,beta.tune*0.9,
                        beta.tune)
)
```

```r
    ##
    ## Save samples
    ##

    phi.save[k,]=phi
    alpha.save[k,]=c(alpha)
    s2.alpha.save[k,]=s2.alpha[1,]
    beta.save[k,]=beta

    ##
    ## Simulate data from model
    ##

    ##
    ## Davg for DIC
    ##

    Davg.save[k]=-2*sum(dpois(Y,as.matrix(H.bd%*%lambda),
                              log=TRUE), na.rm = TRUE)

    if(k%%min(5000,n.iter)==0){
      samples=list(
        phi=phi.save[1:k,],
        phi.tune=phi.tune,
        phi.accept=accept.phi/k,
        alpha=alpha.save[1:k,],
        alpha.tune=alpha.tune,
        alpha.accept=accept.alpha/k,
        s2.alpha=s2.alpha.save[1:k],
        s2.alpha.tune=s2.alpha.tune,
        s2.alpha.accept=accept.s2.alpha/k,
        beta=beta.save[1:k,],
        beta.tune=beta.tune,
        beta.accept=accept.beta/k,
        Davg.save=Davg.save[1:k]
      )
      save(samples,file=paste0("~/Dropbox/SageGrouseProject/PPTLag8year.RData"))
    }
  }
)
beep(6)


###################################################################
### Check convergence
```

```
###############################################################

accept.alpha/k

load(paste0("~/Dropbox/SageGrouseProject/PPTLag8year.RData"))


(n.iter=sum(!is.na(samples$alpha[,1])))
burn=200000
thin=10
ind=seq(burn+1,n.iter,thin)
length(ind)


##
##  Calculate DIC
##


dbar = mean(Davg.save[ind])
post.beta.mn = apply(beta.save[ind,],2,mean)
post.alpha.mn = matrix(apply(alpha.save[ind,],2,mean), 4, T)
post.lambda.mn = exp(X.n%*%post.beta.mn + c(Phi%*%post.alpha.mn))
dhat = -2*sum(dpois(Y,as.matrix(H.bd%*%post.lambda.mn),log= TRUE), na.rm = TRUE)
pd=dbar-dhat
DIC=dhat + 2*pd


##
## Range
##


phi.samp=samples$phi[ind]
tail(phi.samp,1)
plot(phi.samp,type='l')
if(!real.data)abline(h=phi.truth,col=2)
samples$phi.tune
samples$phi.accept
phi.pmed=quantile(phi.samp,0.5)


###
### alpha
###


alpha.samp=samples$alpha[ind,]
dim(alpha.samp)
alpha.samp=samples$alpha[ind,]
par(mfrow = c(4,4), mar = c(4,4,1,1))
```

```
# t=56
for(t in 2:(T-1)){
  plot(alpha.samp[,t*4-3],type='l', main = t)
  if(!real.data)   abline(h=alpha.truth[t*4-3],col=2)
  plot(alpha.samp[,t*4-2],type='l', main = counts.per.month[t])
  if(!real.data)   abline(h=alpha.truth[t*4-2],col=2)
  plot(alpha.samp[,t*4-1],type='l', main = counts.per.month[t])
  if(!real.data)abline(h=alpha.truth[t*4-1],col=2)
  plot(alpha.samp[,t*4],type='l', main = counts.per.month[t])
  if(!real.data) abline(h=alpha.truth[t*4],col=2)
  # readline()
  Sys.sleep(.5)
}


accept.alpha
samples$alpha.tune
samples$alpha.accept
alpha.pmed=matrix(apply(alpha.samp,2,quantile,0.5),n.a,T)


##
## s2.alpha
##

s2.alpha.samp=samples$s2.alpha[ind]
tail(s2.alpha.samp,1)
par(mfrow= c(1,1))
plot(s2.alpha.samp,type='l')
if(!real.data)abline(h=s2.alpha.truth[1],col=2)
samples$s2.alpha.tune
samples$s2.alpha.accept
s2.alpha.pmed=quantile(s2.alpha.samp,0.5)


##
## Beta0
##

beta.samp=samples$beta[ind,]
beta.start=tail(beta.samp,1)
samples$beta.tune
samples$beta.accept
beta.pmed=apply(beta.samp,2,quantile,0.5)


covariate.names=c("elev","slope","bare","sage",
                  "ppt","tmax","burn","ndvi",
                  "pdsi"
```

```
)

par(mfrow=c(2,1))

for(i in 1:ncol(X.m)){

  plot(beta.samp[,i], type='l',main=covariate.names[i],ylim=c(-0.5,0.5))

  if(!real.data)abline(h=beta.truth[i],col=2)

  hist(X.m[,i],main=i)

  readline()

  #Sys.sleep(.5)

}


if(!real.data){

  chk=ifelse(apply(beta.samp,2,quantile,c(0.025,0.975))[1,] < beta.truth&

                apply(beta.samp,2,quantile,c(0.025,0.975))[2,] > beta.truth,1,0)

  mean(chk)

}


######################################################################
### Plot results
######################################################################


trend=matrix(NA,q,length(ind))

x=cbind(1,matrix(1:T,T,1))

lm.f=function(x,y)(solve(t(x)%*%x)%*%t(x)%*%y)[2]

for(k in 1:length(ind)){

  R.k=exp(-D^2/phi.samp[k])

  E.k=eigs_sym(R.k,n.a,which="LM")   # equal to QLQ'

  Phi.k=E.k$vectors%*%diag(E.k$values^(1/2))

  alpha.k=matrix(alpha.samp[k,],n.a,T)

  beta.k=beta.samp[k,]

  lambda.k=matrix(exp(c(Phi.k%*%alpha.k)+X.m%*%beta.k),q,T)

  trend[,k]=apply(lambda.k,1,lm.f,x=x)

  #print(k)

}


mean.trend=apply(trend,1,mean)

mean.trend2=ifelse(mean.trend>0,1,0)

var.trend=apply(trend,1,var)

q.trend=apply(trend,1,quantile,c(0.025,0.975))

certain=ifelse(q.trend[1,]<0&q.trend[2,]>0,NA,1)


levelplot(t(matrix(boundary*mean.trend,nr=ny,nc=nx,byrow=TRUE))[,ny:1],

          cuts = 1000, main = list("Trend",side=1,line=0.5),

          margin = FALSE,

          scales = list(draw = FALSE),

          names.attr = t,
```

```
                at=seq(-0.6,0.5,length.out=800),
                col.regions =colorRampPalette(
                  rev(brewer.pal(11, 'Spectral')),bias = 1)
)


mean(mean.trend)
quantile(mean.trend, c(0.025,0.5,0.975))


levelplot(t(matrix(boundary*mean.trend2,nr=ny,nc=nx,byrow=TRUE))[,ny:1],
                cuts = 1000, main = list("Increasing_or_Decreasing?",side=1,line=0.5),
                margin = FALSE,
                scales = list(draw = FALSE),
                names.attr = t,
                at=seq(min(mean.trend2),max(mean.trend2),length.out=800),
                col.regions =colorRampPalette(
                  rev(brewer.pal(11, 'Spectral')),bias = 1)
)
mean(mean.trend2)
quantile(mean.trend2, c(0.025,0.5,0.975))


levelplot(t(matrix(boundary*mean.trend2*certain,nr=ny,nc=nx,byrow=TRUE))[,ny:1],
                cuts = 1000, main = list("Are_we_sure?",side=1,line=0.5),
                margin = FALSE,
                scales = list(draw = FALSE),
                names.attr = t,
                at=seq(min(mean.trend2),max(mean.trend2),length.out=800),
                col.regions =colorRampPalette(
                  rev(brewer.pal(11, 'Spectral')),bias = 1)
)


levelplot(t(matrix(boundary*var.trend,nr=ny,nc=nx,byrow=TRUE))[,ny:1],
                cuts = 1000, main = list("Variance_in_trend",side=1,line=0.5),
                margin = FALSE,
                scales = list(draw = FALSE),
                names.attr = t,
                at=seq(min(var.trend),max(var.trend),length.out=800),
                col.regions =colorRampPalette(
                  rev(brewer.pal(11, 'Spectral')),bias = 1)
)
mean(var.trend)
quantile(var.trend, c(0.025,0.5,0.975))


###
### Expected count at leks
###
```

```r
phi=phi.pmed
R=exp(-D^2/phi.pmed)
E=eigs_sym(R,n.a,which="LM")
Phi=E$vectors%*%diag(E$values^(1/2),nrow=n.a,ncol=n.a)
s2.alpha=s2.alpha.pmed
lambda=exp(c(Phi%*%alpha.pmed)+X.n%*%beta.pmed)
range(lambda)
marg.lambda=numeric(T)
for(t in 1:T){
  marg.lambda[t]=sum(lambda[ls[t]:le[t]])
}
max(marg.lambda)
par(mfrow=c(1,1))
plot(marg.lambda,type='l')
plot(marg.lambda,type='l', xlab = "Time_period_(months)", ylab = expression(Marginal~Expected~Counts~(lambda)),
     main = "Standardized_Maximum_Lek_Counts_vs._Marginal_Expected_Lek_Counts")


slc=c(12.8,10.4,7.8,12.5,14.5,13.5,14.7,11.8,9,6,8,7.5,9,8,8.4,11,10,9.7,8.5)*q
lines(seq(1,T,12), slc, col=2,lwd=3)
title=expand.grid(month=1:12,year=2000:2018)
year=floor(months.ind/12)+2000
month=round((months.ind/12)%%1*12)
title=paste(year,month,sep="__")


for(t in 1:T){
  pdf(paste0("~/Dropbox/SageGrouseProject/",
             "Images/",t,"_plot.pdf"))
  print(
    levelplot(t(matrix((boundary*lambda[ls[t]:le[t]]),nr=ny,nc=nx,byrow=TRUE))[,ny:1],
              cuts = 1000, main = list(title[t],side=1,line=0.5),
              margin = FALSE,
              scales = list(draw = FALSE),
              names.attr = as.character(t),
              at=seq(min((lambda)),300,length.out=300),
              col.regions =colorRampPalette(
                rev(brewer.pal(11, 'Spectral')),bias = 1)
    )

  )
  ##    dev.off()
  Sys.sleep(1)
}
```